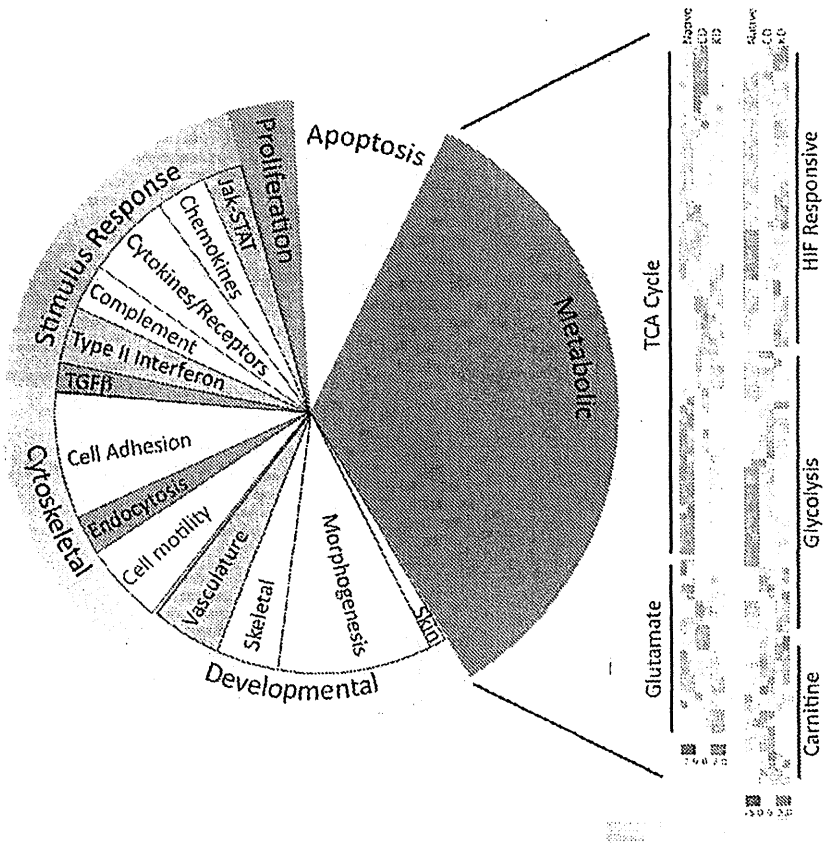

Figure 1: Transcriptomic analysis of human pulmonary microvascular endothelial cells expressing one of two dominant negative BMPR2 mutant constructs. The pie chart depicts the pathways represented by the 507 genes showing significantly altered expression in the CD and KD mutant hPMVEC compared to the native hPMVEC. The largest single major ontology group was metabolic genes, and the heatmap at the right of the figure shows changes in individual genes within this larger group broken down by subsets, with red indicating increased expression and blue denoting decreased expression.

Increased pentose phosphate pathway metabolites and polyamine biosynthesis indicate increased proliferation in BMPR2 mutant endothelial cells

Intermediates in the pentose phosphate pathway for BMPR2 mutant hPMVEC along with changes in the expression of the corresponding genes compared to native hPMVEC are shown (Fig. 2). The pentose phosphate pathway interfaces with multiple other metabolic pathways, including the glycolytic pathway and NADPH synthetic pathways, in addition to providing 5-carbon sugars for nucleotide synthesis. The enzyme primarily responsible for synthesis of NADPH in the pentose phosphate pathway, glucose-6-phosphate dehydrogenase, exhibited significantly reduced expression in both the CD and KD mutants. The upregulation of the pentose phosphate pathway in the BMPR2 mutant hPMVEC thus was apparently driven by upregulation from ribose-5-phosphate isomerase downstream that overcame decreases in glucose-6-phosphate dehydrogenase expression and that directly related to increased nucleotide synthesis and salvage. The significantly increased levels of purine and pyrimidine nucleosides downstream from both mutations further supported this conclusion. Finally, intermediates in the terminal portion of the polyamine synthesis pathway in the CD and KD mutants were increased preferentially over urea cycle intermediates (Figure S3), further supporting the increased cell proliferation previously observed for these specific mutations.[6]

Multiple energy metabolism pathways were disrupted in BMPR2 mutant endothelium

Several groups have previously shown an increase in aerobic glycolysis (the "Warburg effect") in PAH,[7-9,35] and increased glucose uptake has been demonstrated in the lungs of PAH patients by positron emission tomography.[10] In this whole metabolome analysis, glycolysis showed significant upregulation as a consequence of BMPR2 mutation, though this was not to the same extent for both mutations (Fig. 3). Glycolytic metabolites were significantly increased in the CD mutants for all of the pathway intermediates down to pyruvate, whereas the KD mutants showed statistically significant increases or trends in increases only for the metabolites earlier in the glycolytic pathway. Consistent with global activation of the glycolytic pathway, expression of the majority of the genes for glycolytic enzymes was increased, including genes coding for glucose uptake transporters. The genes for two of the three regulated enzymes in the pathway, hexokinase, and phosphofructokinase, showed decreased expression in arrays from the BMPR2 mutant hPMVEC, though the third regulated enzyme, pyruvate kinase, showed increased expression for at least one isoform.

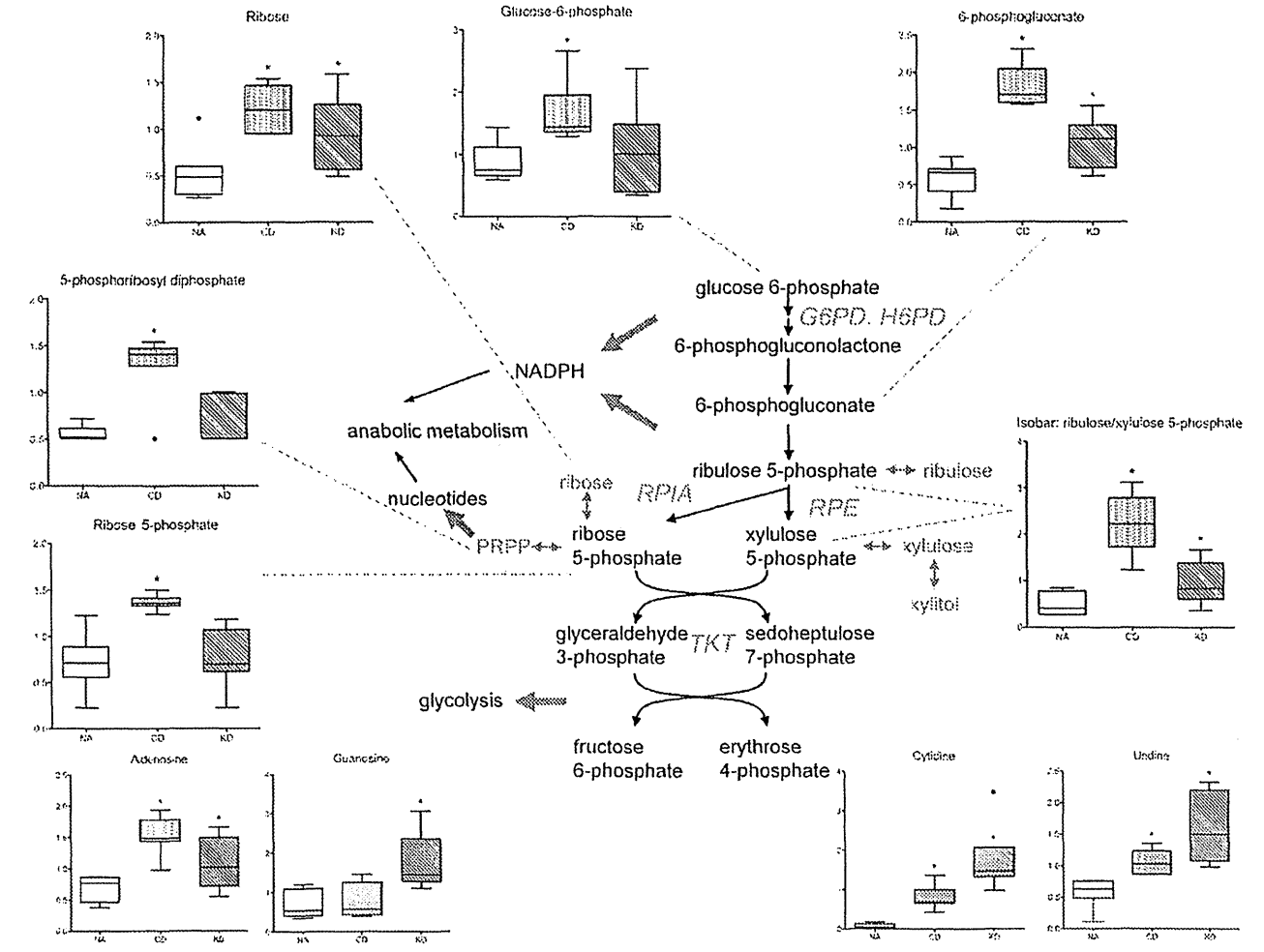

Figure 2: Intermediates in the pentose phosphate pathway specific to nucleotide synthesis are increased in BMPR2 mutant hPMVEC. Major intermediates in the pentose phosphate pathway are shown. In all graphs, native hPMVEC are in white boxes, CD hPMVEC in vertical hatched boxes, and KD hPMVEC in diagonal hatched boxes. Quantities are in arbitrary units specific to the internal standards for each quantified metabolite and normalized to protein concentration. N = 7 for each box, with whiskers indicating Tukey whiskers and extreme data points indicated by filled circles. $^{*}P<0.05$ compared to native. Genes coding for the enzymes that catalyze particular steps in the pathway are indicated by their Entrez Gene names, with red indicating significantly increased expression in the transcriptomic analysis and blue indicating significantly decreased expression. The four graphs at the bottom of the figure show quantitation of purine and pyrimidine nucleosides. G6PD, glucose-6-phosphate dehydrogenase; H6PD, hexose-6-phosphate dehydrogenase; RPIA, ribose-5-phosphate isomerase A; RPE, ribulose-5-phosphate-3-epimerase; TKT, transketolase.

The interplay between fatty acid oxidation and glucose utilization has been shown to play an important role in pulmonary hypertension related to chronic hypoxia and in right ventricular hypertrophy and failure induced by pressure overload in a pulmonary artery banding model,[9,18] but this has not been explored in pulmonary arterial hypertension specifically. We thus sought evidence for alterations in the major pathways for fatty acid oxidative metabolism in the context of disease-causing BMPR2 mutations. We found that carnitine and its downstream acyl metabolites were significantly reduced in the CD and KD mutant hPMVEC compared to the native endothelial cells (Fig. 4). Decreased levels of carnitine itself as well as glycine (a by-product of carnitine synthesis) suggested decreased synthesis of carnitine itself. Levels of palmitoylcarnitine, isobutyrylcarnitine, and propionylcarnitine were also significantly decreased. Decreased expression of many of the key genes involved in carnitine/acylcarnitine metabolism and trafficking was also observed, including the two major carnitine palmitoyltransferase genes and one of the major carnitine/acylcarnitine translocases. We also found significantly decreased expression of a number of the acyl-CoA dehydrogenase genes involved in fatty acid oxidation.

Activity of the tricarboxylic acid (TCA) cycle has been shown to be reduced in a variety of different types of cancer, and this has been proposed to be a central advantage exploited by cancer cells, allowing for diversion of TCA cycle intermediates toward macromolecule synthesis while relying on other energy-generating pathways such as

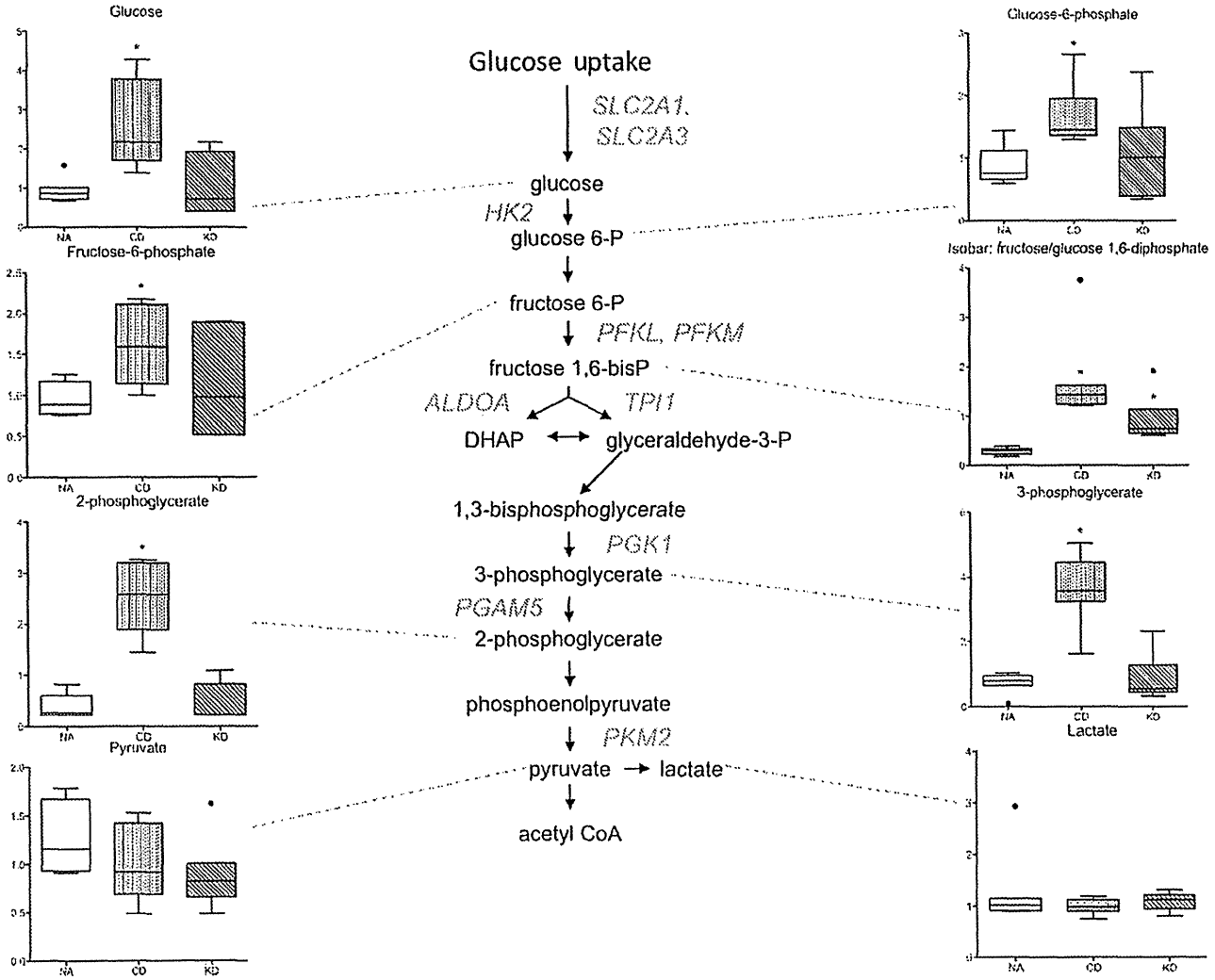

Figure 3: Glycolysis is significantly upregulated in BMPR2 mutant hPMVEC, particularly in cytoplasmic tail domain mutants. The classical glycolysis pathway intermediates are shown. In all graphs, native hPMVEC are in white boxes, CD hPMVEC in vertical hatched boxes, and KD hPMVEC in diagonal hatched boxes. Quantities are in arbitrary units specific to the internal standards for each quantified metabolite and normalized to protein concentration. N = 7 for each box, with whiskers indicating Tukey whiskers and extreme data points indicated by filled circles. *$P < 0.05$ compared to native. Genes coding for the enzymes that catalyze particular steps in the pathway are indicated by their Entrez Gene names, with red indicating significantly increased expression in the transcriptomic analysis and blue indicating significantly decreased expression. *SLC2A1* and *SLC2A3*, solute carrier family 2 (facilitated glucose transporter), members 1 and 3; *HK2*, hexokinase 2; *PFKL* and *PFKM*, phosphofructokinase, liver and muscle isoforms; *ALDOA*, aldolase A; *TPI1*, triosephosphate isomerase 1; *PGK1*, phosphoglycerate kinase 1; *PGAM5*, phosphoglycerate mutase 5; *PKM2*, pyruvate kinase, muscle.

glycolysis.[36-38] Although a number of the metabolic features of cancer cells have been observed in PAH, defects in the TCA cycle have not been extensively described. In hPMVEC expressing BMPR2 mutations, there were extensive metabolic defects in the TCA cycle indicating overall decreased activity of the cycle downstream from citrate (Fig. 5). In particular, significant decreases in succinate, fumarate, and malate were present in the CD mutants, whereas much more mild nonsignificant decreases in the mean concentrations of succinate and malate were observed for the KD mutants. In both mutants, concentrations of citrate were significantly increased, and concentrations of pyruvate and lactate were equivalent to the native hPMVEC, suggesting that the defect in the TCA cycle occurred distal to citrate. Moreover, this suggested that alternative catabolic pathways (e.g., fatty acid oxidation, peptide/amino acid catabolism) feeding into the TCA cycle were insufficient to support concentrations of succinate, fumarate, and malate, particularly in the CD mutants. The balance of TCA cycle intermediates is normally maintained by the complementary processes of anaplerosis and cataplerosis. Broadly defined, anaplerosis refers to the addition of 4- and 5-carbon intermediates into the TCA cycle (e.g., oxaloacetate, alpha-ketoglutarate, and succinyl-CoA) using pyruvate, aspartate, glutamate, or fatty acids as substrates, to support mitochondrial respiration and to replenish TCA cycle intermediates diverted to biosynthesis. Cataplerosis refers to the removal of these same TCA cycle intermediates

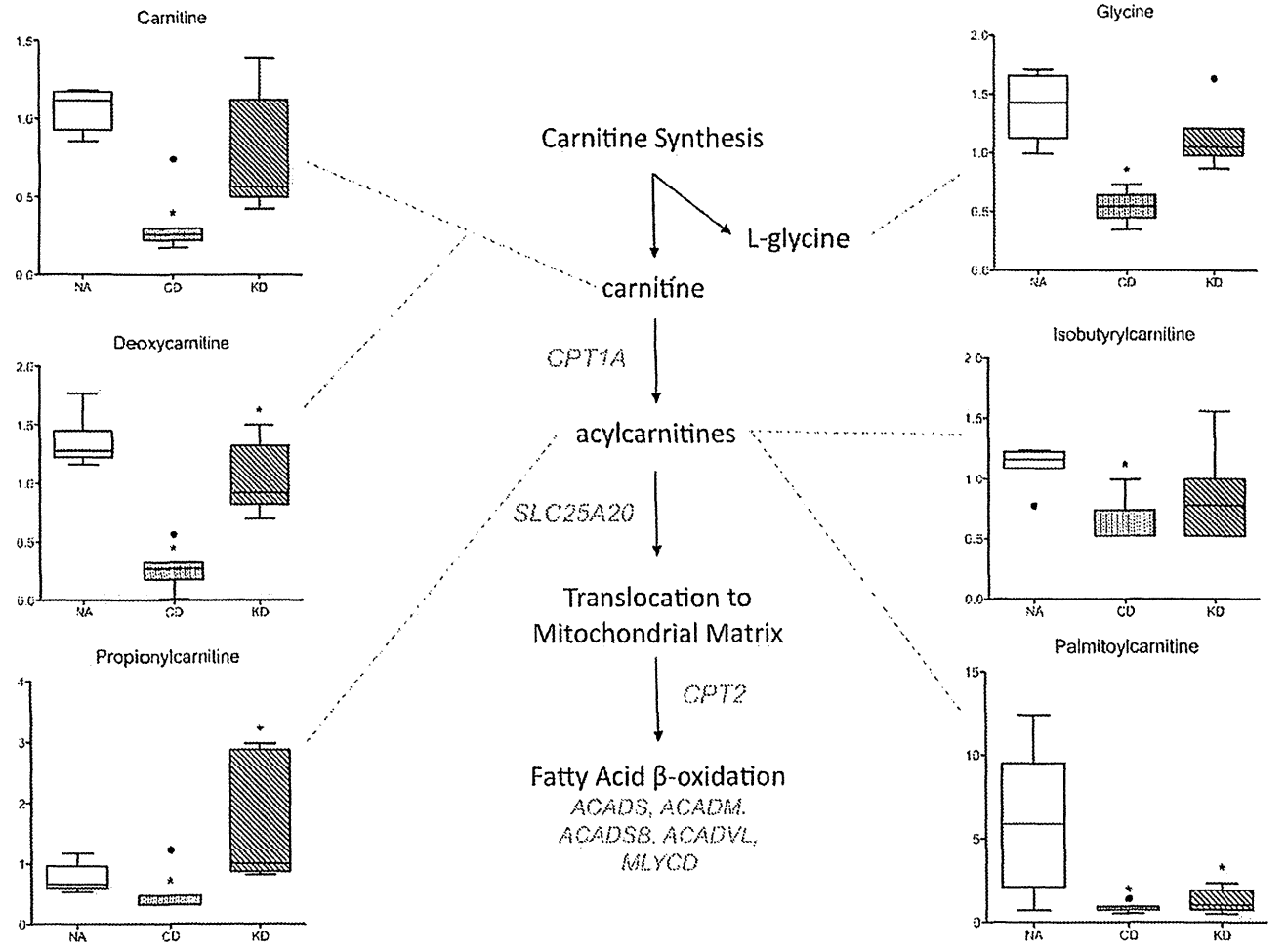

Figure 4: Carnitine metabolism and fatty acid oxidation are significantly depressed in BMPR2 mutant hPMVEC. Multiple carnitine metabolites and their flow into fatty acid oxidation are shown. Intermediates for which significant differences in one or both mutant conditions were detected are shown. In all graphs, native hPMVEC are in white boxes, CD hPMVEC in vertical hatched boxes, and KD hPMVEC in diagonal hatched boxes. Quantities are in arbitrary units specific to the internal standards for each quantified metabolite and normalized to protein concentration. $N = 7$ for each box, with whiskers indicating Tukey whiskers and extreme data points indicated by filled circles. *$P<0.05$ compared to native. Genes coding for the enzymes that catalyze particular steps in the pathway are indicated by their Entrez Gene names, with red indicating significantly increased expression in the transcriptomic analysis and blue indicating significantly decreased expression. CPT1A and CPT2, carnitine palmitoyltransferase isoforms 1A and 2; SLC25A20, carnitine/acylcarnitine translocase; ACADS, ACADM, ACADSB, and ACADVL, acyl-CoA dehydrogenases – short chain, medium chain, short/branched chain, and very long chain; MLYCD, malonyl-CoA decarboxylase

to support biosynthetic processes such as gluconeogenesis, glyceroneogenesis, and fatty acid synthesis.[39]

Two key specific anaplerotic pathways are the conversion of glutamine to glutamate and then to alpha-ketoglutarate, and the conversion of aspartate to oxaloacetate.[40] Levels of these specific amino acids were quantified and found to be significantly reduced in the CD mutant hPMVEC compared to native cells (Fig. 6). By contrast, the KD mutants showed increased levels of glutamine and glutamate, which likely contributed to the more modest reductions of TCA cycle intermediates in these cells, as there was more glutamine and glutamate available for the anaplerotic synthesis of alpha-ketoglutarate. The differences between the CD and KD mutants may be at least in part attributable to differences in the synthesis of N-acetylaspartylglutamate (NAAG). The CD mutants showed increased expression of NAAG synthetase and increased concentrations of NAAG, whereas the KD mutants showed decreased expression of NAAG synthetase and a subsequently lower level of NAAG compared to the CD mutants. It thus is likely that, in the CD mutants, much of the glutamate and aspartate that might otherwise have been used to feed into the TCA cycle was instead being used for the synthesis of NAAG. This was not the case in the KD mutants. Both mutations appeared to drive an overall increase in peptide and amino acid catabolism, as both mutants showed significant increases

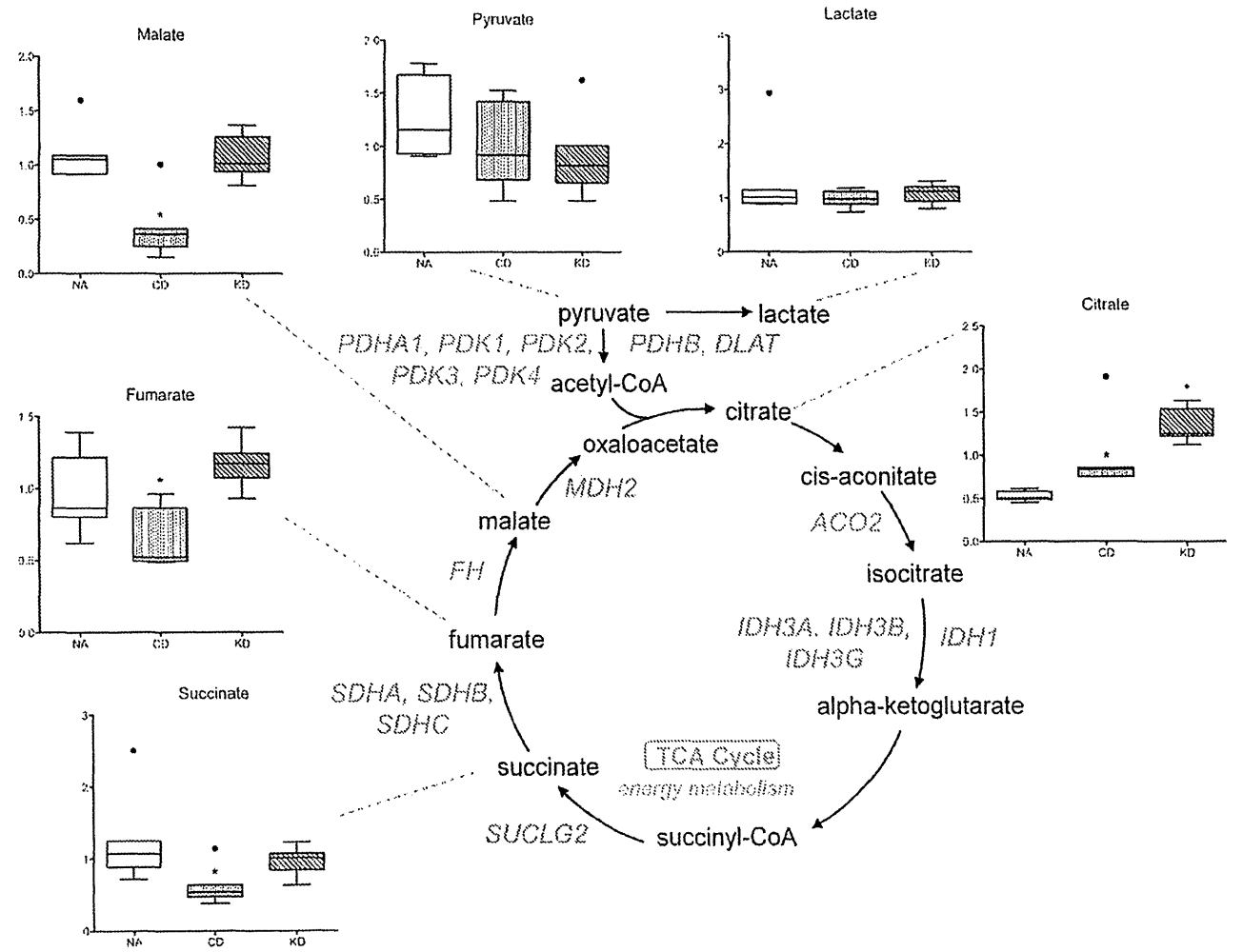

Figure 5: TCA cycle intermediates are significantly decreased in BMPR2 mutant hPMVEC, particularly in CD mutants. The TCA cycle and its major intermediates are shown. In all graphs, native hPMVEC are in white boxes, CD hPMVEC in vertical hatched boxes, and KD hPMVEC in diagonal hatched boxes. Quantities are in arbitrary units specific to the internal standards for each quantified metabolite and normalized to protein concentration. $N = 7$ for each box, with whiskers indicating Tukey whiskers and extreme data points indicated by filled circles. $^{*}P < 0.05$ compared to native. Genes coding for the enzymes that catalyze particular steps in the pathway are indicated by their Entrez Gene names, with red indicating significantly increased expression in the transcriptomic analysis and blue indicating significantly decreased expression. *PDK1-4*, pyruvate dehydrogenase kinase 1-4; *PDHA1*, pyruvate dehydrogenase (lipoamide) alpha 1; *PDHB*, pyruvate dehydrogenase E1 component, beta subunit; *DLAT*, dihydrolipoamide S-acetyltransferase; *ACO2*, aconitase 2; *IDH3A/B/G*, isocitrate dehydrogenase 3 (NAD+) alpha, beta, and gamma subunits; *IDH1*, isocitrate dehydrogenase 1 (NADP+); *SUCLG2*, succinate-CoA ligase, GDP-forming, beta subunit; *SDHA/B/C*, succinate dehydrogenase complex subunits A (flavoprotein), B (iron-sulfur), and C (15kDa integral membrane protein); *FH*, fumarate hydratase; *MDH2*, malate dehydrogenase 2.

in the concentrations of dipeptides (Figure S4), though this was more pronounced in the CD mutants. In addition, anaplerosis via branched chain amino acid metabolism appeared to be more significantly impaired in the CD mutants compared to the KD mutants, as evidenced by more significant decreases in isobutyrylcarnitine and propionylcarnitine, metabolites that participate in branched chain amino acid metabolism as well as fatty acid metabolism. The CD mutants exhibited a major failure of anaplerosis on multiple levels that was much more mild in the KD mutants, and thus must rely on multiple "salvage" pathways of peptide/amino acid catabolism.

Predicted differences in IDH1/2 activity were present in mutant hPMVEC and in human PAH patients

We chose to examine the TCA cycle in more detail, as this is a major point of integration of multiple pathways involved in energy production as well as biosynthesis and so might better reflect the summation of alterations in these many different pathways. On closer inspection of the transcriptomic and metabolomic data relevant to the TCA cycle, there was a clear functional change in the BMPR2 mutants compared to the wild-type endothelial cells that occurred somewhere between citrate and succinate. The two most likely enzymatic candidates were aconitase and

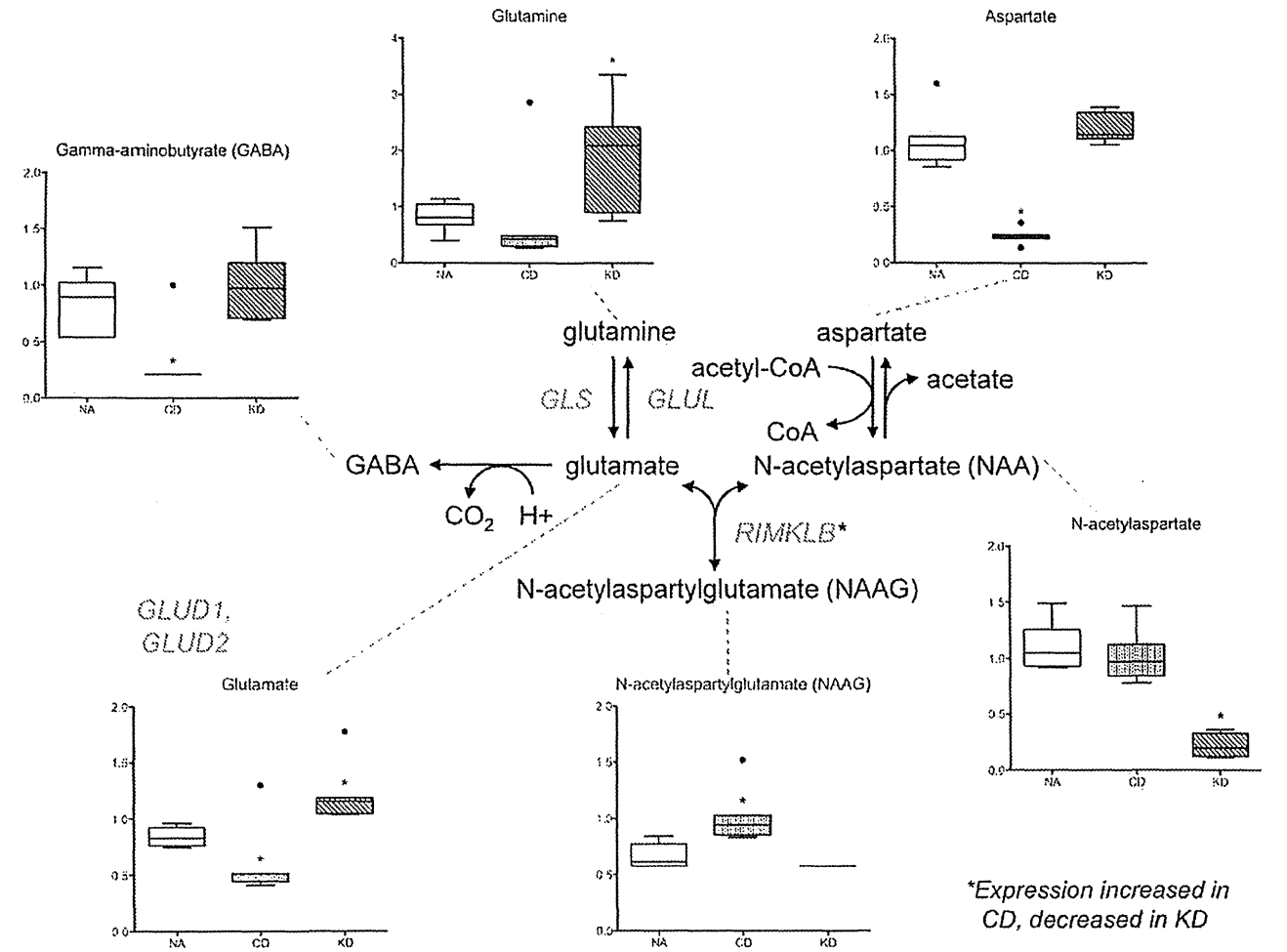

Figure 6: Glutamine/glutamate and aspartate metabolism, two major anaplerotic pathways, are significantly reduced in CD mutant hPMVEC. Intermediates for which significant differences in one or both mutant conditions were detected are shown. In all graphs, native hPMVEC are in white boxes, CD hPMVEC in vertical hatched boxes, and KD hPMVEC in diagonal hatched boxes. Quantities are in arbitrary units specific to the internal standards for each quantified metabolite and normalized to protein concentration. $N = 7$ for each box, with whiskers indicating Tukey whiskers and extreme data points indicated by filled circles. *$P<0.05$ compared to native. Genes coding for the enzymes that catalyze particular steps in the pathway are indicated by their Entrez Gene names, with red indicating significantly increased expression in the transcriptomic analysis and blue indicating significantly decreased expression. GLUD1 and GLUD2, glutamate dehydrogenase 1 and 2; GLS, glutaminase; GLUL, glutamate-ammonia ligase. RIMKLB, N-acetylaspartylglutamate synthetase B.

isocitrate dehydrogenase (IDH). Of these two enzymes, aconitase has been shown to be inactivated by oxidative stress,[41] and oxidative stress is known to be increased in the context of BMPR2 mutations.[22] To remove this as a confounding factor, we chose to examine IDH activity. While NAD^+-dependent IDH activity (corresponding to the IDH3 isoform) did not differ between wild-type and BMPR2 mutant endothelial cells, $NADP^+$-dependent IDH activity (corresponding to IDH isoforms 1 and 2, hereafter IDH1/2) was significantly increased in BMPR2 mutant endothelial cells (Fig. 7A). We then sought to determine if these findings were applicable to patients with PAH. We quantified IDH1/2 activity in serum from controls, from patients with heritable PAH known to have BMPR2 mutations, and from two pooled cohorts of patients with IPAH (one from the United States and one from Japan). Serum IDH1/2 activity was significantly increased in both HPAH and IPAH patients compared to controls (Fig. 7B). The variability in IDH1/2 activity observed in the PAH patients likely does reflect variability in disease activity, at least in part. We separated the PAH patients for whom data were available into two groups based upon the presence or absence of any prostanoid therapy (intravenous, subcutaneous, or inhaled prostacyclin receptor agonist) and analyzed serum IDH1/2 activity (Figure S5). Though only approaching statistical significance ($P=0.1$ by Welch's t-test), the mean serum IDH1/2 activity for the prostanoid treated group of PAH patients clearly trended toward being higher than for the nontreated group. As prostanoid therapy is only initiated in more severe disease, the higher serum IDH activity may well be a reflection of disease severity.

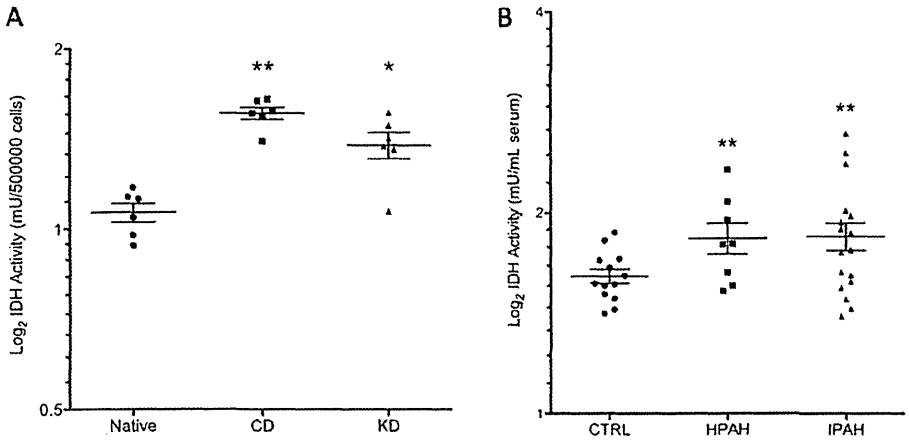

Figure 7: IDH1/2 activity is increased in mutant hPMVEC and in serum from patients with pulmonary arterial hypertension. (A) Compared to native hPMVEC (1.07±0.04 mU/5×10⁵ cells), the CD and KD mutant-expressing hPMVEC both show significantly increased NADP⁺-dependent IDH activity in cell lysates (1.56±0.04 and 1.38 +/ 0.07 mU/5 · 10⁵ cells, respectively). N=6 for each group, mean±SEM indicated. $P<0.0001$ by one-way ANOVA, $^{**}P<0.0001$ vs. native. $^{*}P<0.003$ vs. native. (B) NADP⁺-dependent IDH activity in the serum from patients with heritable PAH (N=8, 1.83±0.1 mU/mL) and idiopathic PAH (N=17, 1.85±0.09 mU/mL) was significantly increased compared to serum from normal control individuals (N=13, 1.61±0.04 mU/mL), mean±SEM indicated. $^{**}P<0.03$ vs. control by Welch's t-test.

DISCUSSION

We present here a whole metabolome analysis of the effects of BMPR2 mutations known to cause pulmonary arterial hypertension. We have constructed an integrated picture of the complex and interdependent metabolic changes that occur downstream from BMPR2 mutations in human pulmonary microvascular endothelial cells, and this integrated view has demonstrated more widespread metabolic defects in PAH than have been previously known. The shift toward aerobic glycolysis that is typified by the Warburg effect in PAH has been known for some time.[7] More recently, the interplay between fatty acid oxidation and control of glycolysis versus glucose oxidation (typified by the Randle cycle) has been demonstrated to be important in hypoxic pulmonary hypertension.[9,42] In addition to confirming these previously identified metabolic defects in PAH, we have identified significant alterations in the TCA cycle and at least some of the pathways that interact with it.

Our analysis reveals a profound failure of anaplerosis present downstream from BMPR2 mutations that has been largely unexplored as a mechanism of disease pathogenesis in PAH. TCA cycle intermediates are depleted through what appears to be a combination of decreased activity of the cycle itself plus abnormal shunting of intermediates from other pathways (e.g., glutamate, glutamine, aspartate, and branched chain amino acids) that could otherwise be used to replenish the intermediates of the TCA cycle. This implies that the metabolic defects in PAH cannot be simply summed up under the umbrella of Warburg metabolism.[35,43] It is possible that diversion of TCA cycle intermediates for biosynthesis and reliance on aerobic glycolysis is actually a feature of decreased BMP signaling, as would be seen in settings of tissue remodeling and repair, for example. However, these would be settings of temporary loss or reduction of BMP signaling, and what might be adaptive cataplerosis in the short-term becomes pathogenic in the setting of permanently decreased BMP signaling due to mutation. More importantly, the therapeutic implication is that it is very likely that most or all of the errant pathways will need to be targeted to expect a significant therapeutic impact, and current investigational therapies address only certain dysfunctional pathways that largely do not address the failure of anaplerosis.

To demonstrate further the utility of our combined metabolomic and transcriptomic analysis, we chose to quantify NADP⁺-dependent IDH activity. We predicted that this enzymatic activity would be altered in PAH and then demonstrated the accuracy of that prediction in both cultured cells and in patients with PAH. Alterations in IDH activity have not been previously described in PAH; however, multiple conceptual links between PAH and cancer have been proposed, and there is a growing body of literature linking altered IDH activity in a causative way to at least certain types of cancer,[24,44-47] so the identification of altered IDH1/2 activity in PAH may in fact be directly related to disease pathogenesis.

A second possibility is that the anaplerotic failure and increased IDH1/2 activities in PAH are driving forces for HIF activation that underlies PAH,[15,48] which then perpetuates increased aerobic glycolysis, apoptosis resistance, and decreased mitochondrial number.[11] HIF can be activated by decreased alpha-ketoglutarate and increased citrate concentrations, both of which activate

HIF by decreasing the efficiency of prolyl hydroxylase.[49] Under hypoxic conditions, activation of HIF has very recently been shown to increase IDH2-mediated conversion of glutamine-derived alpha-ketoglutarate to citrate.[50] The resultant hypothesized increase in citrate and decrease in alpha-ketoglutarate brought about by increased IDH2 activity would thus be predicted to further drive HIF activation, setting up something of a vicious cycle. Our data show significant changes in the expression of HIF responsive genes in BMPR2 mutant hPMVEC. Alternatively, HIF activation can be driven by increased oxidative stress and decreased antioxidant defenses, as is seen with epigenetic inactivation of SOD2,[51] and this may be the upstream event that drives IDH activation. HIF activation can drive metabolic reprogramming that leads to increased IDH activity,[50] and IDH may be upregulated in response to oxidative stress to serve as a source of NADPH that is used to maintain reduced glutathione pools intracellularly.[52]

More importantly, IDH activity appears to track with disease activity, as patients with more severe disease (i.e., those treated with a prostacyclin agonist) trend toward higher serum IDH activity. The fact that those patients with disease severe enough to warrant prostanoid therapy still exhibit increased serum IDH activity after the initiation of therapy suggests that our most efficacious class of drugs for PAH still does not correct all of the underlying metabolic defects in PAH and highlights the need for therapies that arise from a deeper understanding of the molecular pathogenesis of PAH. Further investigations are needed to determine if the increased IDH activity described in PAH in this study is truly pathogenic, adaptive, or epiphenomenon.

This type of investigation is not without limitations. The pulmonary endothelial cell clearly plays an important role in the pathogenesis of PAH, but many other cell types, including smooth muscle cells,[53] lung mesenchymal stem cells,[54] and resident immune cells[55] all likely contribute to disease development. It is not possible in most cases in this study to determine what changes are truly causative of disease and which are consequences of the disease, although examination of cells in culture minimizes this problem to some degree.[23] While identification of putative molecular targets is possible and is greatly enhanced by this type of layered analysis, each target must be further validated independently and placed into a context. Still, this study has permitted the identification of previously unrecognized pathways that likely directly contribute to the development of PAH; the identification of promising new biomarkers, of which IDH1/2 activity is but one, to guide diagnosis and therapeutic evaluation; and the recognition of the importance of defining and simultaneously targeting the multiple affected metabolic pathways in future therapeutic development. We hypothesize that this approach would be similarly fruitful in many other complex diseases.

APPENDIX

Supplemental Methods

Metabolomic Analysis: Native and mutant hPMVEC were grown to 80% confluence (yielding approximately 1-3 $\times 10^7$ cells per sample), transitioned from G418 sulfate selection to complete media without antibiotic for at least 12 hours, and washed with phosphate-buffered saline and trypsinized to harvest cells. Cells were pelleted, the supernatant removed, and the dry pellet snap frozen in liquid nitrogen and stored at -80C until analysis. The non-targeted metabolic profiling platform employed for this analysis combined three independent platforms: ultrahigh performance liquid chromatography/tandem mass spectrometry (UHPLC/MS/MS^2) optimized for basic species, UHPLC/MS/MS^2 optimized for acidic species, and gas chromatography/mass spectrometry (GC/MS). Samples were processed essentially as described previously.[1,2] For each sample, 100L was used for analyses. Using an automated liquid handler (Hamilton LabStar, Salt Lake City, UT), protein was precipitated from the homogenate with methanol that contained four standards to report on extraction efficiency. The resulting supernatant was split into equal aliquots for analysis on the three platforms. Aliquots, dried under nitrogen and vacuum-desiccated, were subsequently either reconstituted in 50L 0.1% formic acid in water (acidic conditions) or in 50L 6.5mM ammonium bicarbonate in water, pH 8 (basic conditions) for the two UHPLC/MS/MS^2 analyses or derivatized to a final volume of 50L for GC/MS analysis using equal parts bistrimethyl-silyl-trifluoroacetamide and solvent mixture acetonitrile:dichloromethane:cyclohexane (5:4:1) with 5% triethylamine at 60°C for one hour. In addition, three types of controls were analyzed in concert with the experimental samples: aliquots of a well-characterized human plasma pool served as technical replicates throughout the data set, extracted water samples served as process blanks, and a cocktail of standards spiked into every analyzed sample allowed instrument performance monitoring. Experimental samples and controls were randomized across platform run days.

For UHLC/MS/MS^2 analysis, aliquots were separated using a Waters Acquity UPLC (Waters, Millford, MA) and analyzed using an LTQ mass spectrometer (Thermo Fisher Scientific, Inc., Waltham, MA) which consisted of an electrospray ionization (ESI) source and linear ion-trap (LIT) mass analyzer. The MS instrument scanned 99-1000 m/z and alternated between MS and MS^2 scans

using dynamic exclusion with approximately 6 scans per second. Derivatized samples for GC/MS were separated on a 5% phenyldimethyl silicone column with helium as the carrier gas and a temperature ramp from 60°C to 340°C and then analyzed on a Thermo-Finnigan Trace DSQ MS (Thermo Fisher Scientific, Inc.) operated at unit mass resolving power with electron impact ionization and a 50-750 atomic mass unit scan range.

Metabolites were identified by automated comparison of the ion features in the experimental samples to a reference library of chemical standard entries that included retention time, molecular weight (m/z), preferred adducts, and in-source fragments as well as associated MS spectra, and were curated by visual inspection for quality control using software developed at Metabolon.[3]

For statistical analyses and data display purposes, any missing values were assumed to be below the limits of detection and these values were imputed with the compound minimum (minimum value imputation). Statistical analysis of log-transformed data was performed using "R" (http://cran.r-project.org/). Welch's t-tests were performed to compare data between experimental groups. A p-value of < 0.05 was considered statistically significant and multiple comparisons were accounted for by estimating the false discovery rate (FDR) using q-values.[4]

REFERENCES

1. Runo JR, Loyd JE. Primary pulmonary hypertension. Lancet 2003;361:1533-44.
2. Agarwal R, Gomberg-Maitland M. Current therapeutics and practical management strategies for pulmonary arterial hypertension. Am Heart J 2011;162:201-13.
3. Liu D, Liu QQ, Eyries M, Wu WH, Yuan P, Zhang R, et al. Molecular genetics and clinical features of Chinese IPAH and HPAH patients. Eur Respir J 2012;39:597-603.
4. Dewachter L, Adnot S, Guignabert C, Tu L, Marcos E, Fadel E, et al. Bone morphogenetic protein signalling in heritable versus idiopathic pulmonary hypertension. Eur Respir J 2009;34:1100-10.
5. Austin ED, Menon S, Hemnes AR, Robinson LJ, Talati M, Fox KL, et al. Idiopathic and heritable PAH perturb common molecular pathways, correlated with increased MSX1 expression. Pulm Circ 2011;1:389-98.
6. Majka S, Hagen M, Blackwell T, Harral J, Johnson JA, Gendron R, et al. Physiologic and molecular consequences of endothelial Bmpr2 mutation. Respir Res 2011;12:84.
7. Rehman J, Archer SL. A proposed mitochondrial-metabolic mechanism for initiation and maintenance of pulmonary arterial hypertension in fawn-hooded rats: The Warburg model of pulmonary arterial hypertension. Adv Exp Med Biol 2010;661:171-85.
8. Piao L, Marsboom G, Archer SL. Mitochondrial metabolic adaptation in right ventricular hypertrophy and failure. J Mol Med (Berl) 2010;88:1011-20.
9. Sutendra G, Bonnet S, Rochefort G, Haromy A, Folmes KD, Lopaschuk GD, et al. Fatty acid oxidation and malonyl-CoA decarboxylase in the vascular remodeling of pulmonary hypertension. Sci Transl Med 2010;2:44ra58.
10. Xu W, Koeck T, Lara AR, Neumann D, DiFilippo FP, Koo M, et al. Alterations of cellular bioenergetics in pulmonary artery endothelial cells. Proc Natl Acad Sci U S A 2007;104:1342-7.
11. Fijalkowska I, Xu W, Comhair SA, Janocha AJ, Mavrakis LA, Krishnamachary B, et al. Hypoxia inducible-factor1alpha regulates the metabolic shift of pulmonary hypertensive endothelial cells. Am J Pathol 2010;176:1130-8.
12. Pugh ME, Robbins IM, Rice TW, West J, Newman JH, Hemnes AR. Unrecognized glucose intolerance is common in pulmonary arterial hypertension. J Heart Lung Transplant 2011;30:904-11.
13. Hansmann G, Wagner RA, Schellong S, Perez VA, Urashima T, Wang L, et al. Pulmonary arterial hypertension is linked to insulin resistance and reversed by peroxisome proliferator-activated receptor-gamma activation. Circulation 2007;115:1275-84.
14. Archer SL, Gomberg-Maitland M, Maitland ML, Rich S, Garcia JG, Weir EK. Mitochondrial metabolism, redox signaling, and fusion: A mitochondria-ROS-HIF-1alpha-Kv1.5 O2-sensing pathway at the intersection of pulmonary hypertension and cancer. Am J Physiol Heart Circ Physiol 2008;294:H570-8.
15. Bonnet S, Michelakis ED, Porter CJ, Andrade-Navarro MA, Thebaud B, Haromy A, et al. An abnormal mitochondrial-hypoxia inducible factor-1alpha-Kv channel pathway disrupts oxygen sensing and triggers pulmonary arterial hypertension in fawn hooded rats: similarities to human pulmonary arterial hypertension. Circulation 2006;113:2630-41.
16. McMurtry MS, Bonnet S, Wu X, Dyck JR, Haromy A, Hashimoto K, et al. Dichloroacetate prevents and reverses pulmonary hypertension by inducing pulmonary artery smooth muscle cell apoptosis. Circ Res 2004;95:830-40.
17. Michelakis ED, McMurtry MS, Wu XC, Dyck JR, Moudgil R, Hopkins TA, et al. Dichloroacetate, a metabolic modulator, prevents and reverses chronic hypoxic pulmonary hypertension in rats: Role of increased expression and activity of voltage-gated potassium channels. Circulation 2002;105:244-50.
18. Fang YH, Piao L, Hong Z, Toth PT, Marsboom G, Bache-Wiig P, et al. Therapeutic inhibition of fatty acid oxidation in right ventricular hypertrophy: Exploiting Randle's cycle. J Mol Med (Berl) 2012;90:31-43.
19. Krump-Konvalinkova V, Bittinger F, Unger RE, Peters K, Lehr HA, Kirkpatrick CJ. Generation of human pulmonary microvascular endothelial cell lines. Lab Invest 2001;81:1717-27.
20. Shen JS, Meng XL, Schiffmann R, Brady RO, Kaneski CR. Establishment and characterization of Fabry disease endothelial cells with an extended lifespan. Mol Genet Metab 2007;92:137-44.
21. Abdallah BM, Haack-Sorensen M, Burns JS, Elsnab B, Jakob F, Hokland P, et al. Maintenance of differentiation potential of human bone marrow mesenchymal stem cells immortalized by human telomerase reverse transcriptase gene despite [corrected] extensive proliferation. Biochem Biophys Res Commun 2005;326:527-38.
22. Lane KL, Talati M, Austin E, Hemnes AR, Johnson JA, Fessel JP, et al. Oxidative injury is a common consequence of BMPR2 mutations. Pulm Circ 2011;1:72-83.
23. West J, Cogan J, Geraci M, Robinson L, Newman J, Phillips JA, et al. Gene expression in BMPR2 mutation carriers with and without evidence of pulmonary arterial hypertension suggests pathways relevant to disease penetrance. BMC Med Genomics 2008;1:45.
24. Reitman ZJ, Jin G, Karoly ED, Spasojevic I, Yang J, Kinzler KW, et al. Profiling the effects of isocitrate dehydrogenase 1 and 2 mutations on the cellular metabolome. Proc Natl Acad Sci U S A 2011;108:3270-5.
25. Sreekumar A, Poisson LM, Rajendiran TM, Khan AP, Cao Q, Yu J, et al. Metabolomic profiles delineate potential role for sarcosine in prostate cancer progression. Nature 2009;457:910-4.
26. Dehaven CD, Evans AM, Dai H, Lawton KA. Organization of GC/MS and LC/MS metabolomics data into chemical libraries. J Cheminform 2010;2:9.
27. Storey JD, Tibshirani R. Statistical significance for genomewide studies. Proc Natl Acad Sci U S A 2003;100:9440-5.
28. Rudarakanchana N, Flanagan JA, Chen H, Upton PD, Machado R, Patel D, et al. Functional analysis of bone morphogenetic protein type II receptor mutations underlying primary pulmonary hypertension. Hum Mol Genet 2002;11:1517-25.
29. Foletta VC, Lim MA, Soosairajah J, Kelly AP, Stanley EG, Shannon M, et al. Direct signaling by the BMP type II receptor via the cytoskeletal regulator LIMK1. J Cell Biol 2003;162:1089-98.
30. Machado RD, Rudarakanchana N, Atkinson C, Flanagan JA, Harrison R, Morrell NW, et al. Functional interaction between BMPR-II and Tctex-1, a light chain of Dynein, is isoform-specific and disrupted by mutations underlying primary pulmonary hypertension. Hum Mol Genet 2003;12:3277-86.
31. Wong WK, Knowles JA, Morse JH. Bone morphogenetic protein receptor type II C-terminus interacts with c-Src: implication for a role in pulmonary arterial hypertension. Am J Respir Cell Mol Biol 2005;33:438-46.
32. West J, Fagan K, Steudel W, Fouty B, Lane K, Harral J, et al. Pulmonary hypertension in transgenic mice expressing a dominant-negative BMPRII gene in smooth muscle. Circ Res 2004;94:1109-14.

33. Tada Y, Majka S, Carr M, Harral J, Crona D, Kuriyama T, et al. Molecular effects of loss of BMPR2 signaling in smooth muscle in a transgenic mouse model of PAH. Am J Physiol Lung Cell Mol Physiol 2007;292:L1556-63.
34. West J, Harral J, Lane K, Deng Y, Ickes B, Crona D, et al. Mice expressing BMPR2R899X transgene in smooth muscle develop pulmonary vascular lesions. Am J Physiol Lung Cell Mol Physiol 2008;295:L744-55.
35. Vander Heiden MG, Cantley LC, Thompson CB. Understanding the Warburg effect: the metabolic requirements of cell proliferation. Science 2009;324:1029-33.
36. Reitman ZJ, Yan H. Isocitrate dehydrogenase 1 and 2 mutations in cancer: alterations at a crossroads of cellular metabolism. J Natl Cancer Inst 2010;102:932-41.
37. Tong WH, Sourbier C, Kovtunovych G, Jeong SY, Vira M, Ghosh M, et al. The glycolytic shift in fumarate-hydratase-deficient kidney cancer lowers AMPK levels, increases anabolic propensities and lowers cellular iron levels. Cancer Cell 2011;20:315-27.
38. Possemato R, Marks KM, Shaul YD, Pacold ME, Kim D, Birsoy K, et al. Functional genomics reveal that the serine synthesis pathway is essential in breast cancer. Nature 2011;476:346-50.
39. Owen OE, Kalhan SC, Hanson RW. The key role of anaplerosis and cataplerosis for citric acid cycle function. J Biol Chem 2002;277:30409-12.
40. Scott DA, Richardson AD, Filipp FV, Knutzen CA, Chiang GG, Ronai ZA, et al. Comparative metabolic flux profiling of melanoma cell lines: beyond the Warburg effect. J Biol Chem 2011;9:42626-34.
41. Shiva S, Sack MN, Greer JJ, Duranski M, Ringwood LA, Burwell L, et al. Nitrite augments tolerance to ischemia/reperfusion injury via the modulation of mitochondrial electron transfer. J Exp Med 2007;204:2089-102.
42. Dyck JR, Hopkins TA, Bonnet S, Michelakis ED, Young ME, Watanabe M, et al. Absence of malonyl coenzyme A decarboxylase in mice increases cardiac glucose oxidation and protects the heart from ischemic injury. Circulation 2006;114:1721-8.
43. Tuder RM, Davis LA, Graham BB. Targeting Energetic Metabolism: A new frontier in the pathogenesis and treatment of pulmonary hypertension. Am J Respir Crit Care Med 2012;185:260-6.
44. Yan H, Parsons DW, Jin G, McLendon R, Rasheed BA, Yuan W, et al. IDH1 and IDH2 mutations in gliomas. N Engl J Med 2009;360:765-73.
45. Kil IS, Kim SY, Lee SJ, Park JW. Small interfering RNA-mediated silencing of mitochondrial NADP+-dependent isocitrate dehydrogenase enhances the sensitivity of HeLa cells toward tumor necrosis factor-alpha and anticancer drugs. Free Radic Biol Med 2007;43:1197-207.
46. Figueroa ME, Abdel-Wahab O, Lu C, Ward PS, Patel J, Shih A, et al. Leukemic IDH1 and IDH2 mutations result in a hypermethylation phenotype, disrupt TET2 function, and impair hematopoietic differentiation. Cancer Cell 2010;18:553-67.
47. Amary MF, Bacsi K, Maggiani F, Damato S, Halai D, Berisha F, et al. IDH1 and IDH2 mutations are frequent events in central chondrosarcoma and central and periosteal chondromas but not in other mesenchymal tumours. J Pathol 2011;224:334-43.
48. Tuder RM, Chacon M, Alger L, Wang J, Taraseviciene-Stewart L, Kasahara Y, et al. Expression of angiogenesis-related molecules in plexiform lesions in severe pulmonary hypertension: evidence for a process of disordered angiogenesis. J Pathol 2001;195:367-74.
49. Raimundo N, Baysal BE, Shadel GS. Revisiting the TCA cycle: Signaling to tumor formation. Trends Mol Med 2011;17:641-9.
50. Wise DR, Ward PS, Shay JE, Cross JR, Gruber JJ, Sachdeva UM, et al. Hypoxia promotes isocitrate dehydrogenase-dependent carboxylation of alpha-ketoglutarate to citrate to support cell growth and viability. Proc Natl Acad Sci U S A 2011;108:19611-6.
51. Archer SL, Marsboom G, Kim GH, Zhang HJ, Toth PT, Svensson EC, et al. Epigenetic attenuation of mitochondrial superoxide dismutase 2 in pulmonary arterial hypertension: a basis for excessive cell proliferation and a new therapeutic target. Circulation 2010;121:2661-71.
52. Rydstrom J. Mitochondrial NADPH, transhydrogenase and disease. Biochim Biophys Acta 2006;1757:721-6.
53. Marsboom G, Wietholt C, Haney CR, Toth PT, Ryan JJ, Morrow E, et al. Lung 18F-Fluorodeoxyglucose positron emission tomography for diagnosis and monitoring of pulmonary arterial hypertension. Am J Respir Crit Care Med 2012;185:670-9.
54. Chow KS, Jun D, Helm KM, Wagner DH, Majka SM. Isolation & characterization of Hoechst(low) CD45(negative) mouse lung mesenchymal stem cells. J Vis Exp 2011:e3159.
55. Vergadi E, Chang MS, Lee C, Liang OD, Liu X, Fernandez-Gonzalez A, et al. Early macrophage recruitment and alternative activation are critical for the later development of hypoxia-induced pulmonary hypertension. Circulation 2011;123:1986-95.

SUPPLEMENTAL REFERENCES

1. Ohta T, Masutomi N, Tsutsui N, Sakairi T, Mitchell M, Milburn MV, Ryals JA, Beebe KD, Guo L. Untargeted metabolomic profiling as an evaluative tool of fenofibrate-induced toxicology in Fischer 344 male rats. *Toxicol Pathol.* 2009;37(4):521-535.
2. Evans AM, DeHaven CD, Barrett T, Mitchell M, Milgram E. Integrated, nontargeted ultrahigh performance liquid chromatography/electrospray ionization tandem mass spectrometry platform for the identification and relative quantification of the small-molecule complement of biological systems. *Anal Chem.* Aug 15 2009;81(16):6656-6667.
3. Dehaven CD, Evans AM, Dai H, Lawton KA. Organization of GC/MS and LC/MS metabolomics data into chemical libraries. *J Cheminform.* 2010;2(1):9.
4. Storey JD, Tibshirani R. Statistical significance for genomewide studies. *Proc Natl Acad Sci U S A.* Aug 5 2003;100(16):9440-9445.

Source of Support: This work was supported in part by the Vanderbilt Clinical and Translational Science Awards grant UL1 RR024975-01 from the National Center for Research Resources/NIH, by support provided to JPF by NIH training grant T32 HL094296-02, and by R01 HL095797-01A2 (JW)., **Conflict of Interest:** None declared.

Long-term outcome after pulmonary endarterectomy for chronic thromboembolic pulmonary hypertension

Keiichi Ishida, MD, PhD,[a] Masahisa Masuda, MD, PhD,[c] Nobuhiro Tanabe, MD, PhD,[b] Goro Matsumiya, MD, PhD,[a] Koichiro Tatsumi, MD, PhD,[b] and Nobuyuki Nakajima, MD, PhD[a]

Objectives: Pulmonary endarterectomy is the treatment of choice for chronic thromboembolic pulmonary hypertension. Although several reports demonstrated excellent medium-term survival after pulmonary endarterectomy, long-term outcomes remain unclear. We reviewed long-term outcomes and determined risk factors for early and late adverse events.

Methods: Seventy-seven patients were studied. Mean pulmonary arterial pressure was 47 ± 10 mm Hg and pulmonary vascular resistance was 868 ± 319 dyne · s · cm^{-5}. Disease was classified as chronic thromboembolic pulmonary hypertension type 1 (n = 61), type 2 (n = 12), or type 3 (n = 4). Median and maximum follow-up periods were 5.6 and 20 years, respectively.

Results: There were 11 in-hospital deaths. Nonsurvivors had significantly higher mean pulmonary arterial pressure and pulmonary vascular resistance than did survivors (54 ± 10 vs 46 ± 10 mm Hg; $P = .02$; 1124 ± 303 vs 824 ± 303 dyne · s · cm^{-5}; $P < .01$). In multivariate analysis, preoperative pulmonary vascular resistance was associated with in-hospital death (odds ratio, 1.003; 95% confidence interval, 1.001–1.005; $P < .01$). During follow-up, there were 10 all-cause deaths, including 5 related to chronic thromboembolic pulmonary hypertension. Freedom from adverse events, including disease-specific death or New York Heart Association functional class III, was 70% at 10 years. In the Cox proportional hazard model, postoperative mean pulmonary arterial pressure was associated with adverse events (hazard ratio, 1.12; 95% confidence interval, 1.03–1.21; $P < .01$). Receiver operating characteristic curve analysis showed mean pulmonary arterial pressure of 34 mm Hg as cutoff for adverse events.

Conclusions: Pulmonary endarterectomy had sustained favorable effects on long-term survival. High pulmonary vascular resistance was associated with in-hospital death, and postoperative mean pulmonary arterial pressure was an independent predictor of adverse events. (J Thorac Cardiovasc Surg 2012;144:321-6)

Chronic thromboembolic pulmonary hypertension (CTEPH) is a life-threatening disease caused by unresolved, organized thrombi obstructing the pulmonary arteries.[1,2] Progressive pulmonary hypertension severely compromises both clinical functional status and exercise capacity as a result of ventilation–perfusion mismatch and decreased cardiac output. In patients who do not undergo operation, the prognosis is disappointing and is determined by the severity of the pulmonary hypertension: if mean pulmonary arterial pressure (mPAP) exceeds 30 mm Hg, the 5-year survival is less than 30%, and if it exceeds 50 mm Hg, the 5-year survival is as low as 10%.[3]

Pulmonary endarterectomy (PEA), which has been established as a standard surgical treatment for CTEPH, is performed worldwide, mostly at centers with experience.[1,4] PEA offers immediate and substantial decreases in both mPAP and pulmonary vascular resistance (PVR) and an increase in the cardiac index.[4,5] Medium-term follow-up results for PEA reveal favorable effects on survival and clinical functional status[6-10]; however, the long-term outcomes remain unclear because of the limited available data. We began our PEA program in 1986 and have thus been performing the operation now for more than 20 years. Early on in our series, we performed PEA through a lateral thoracotomy; however, we have performed PEA through median sternotomy with intermittent deep hypothermic circulatory arrest according to the San Diego group procedure since 1990.[4,11,12] Here we review the long-term follow-up outcomes of a consecutive series of patients who underwent PEA through median sternotomy, and we seek to determine the factors influencing both early and late survival and functional status.

MATERIALS AND METHODS

Between 1990 and 2010, a total of 77 patients underwent PEA at Chiba University Hospital and affiliated hospitals. We retrospectively reviewed

From the Departments of Cardiovascular Surgery[a] and Respirology,[b] Graduate School of Medicine, Chiba University, Chiba, Japan; and the Department of Cardiovascular Surgery,[c] National Hospital Organization, Chiba Medical Center, Chiba, Japan.

Disclosures: Authors have nothing to disclose with regard to commercial support.
Received for publication May 28, 2011; revisions received Aug 9, 2011; accepted for publication Sept 15, 2011; available ahead of print Oct 12, 2011.

Address for reprints: Keiichi Ishida, MD, PhD, Department of Cardiovascular Surgery, Graduate School of Medicine, Chiba University, 1-8-1 Inohana Chuo-ku Chiba, 260-8670, Japan (E-mail: keiichi-ishida@pro.odn.ne.jp).

0022-5223/$36.00

doi:10.1016/j.jtcvs.2011.09.004

Abbreviations and Acronyms

CTEPH = chronic thromboembolic pulmonary hypertension
mPAP = mean pulmonary arterial pressure
NYHA = New York Heart Association
PEA = pulmonary endarterectomy
PVR = pulmonary vascular resistance

this cohort of patients. All 77 patients in our cohort underwent preoperative pulmonary angiography, right heart catheterization, and computed tomographic scan. Surgical indications were decided as follows: PVR greater than 300 dyne · s · cm^{-5}, mPAP greater than 30 mm Hg, New York Heart Association (NYHA) functional class greater than II, and absence of significant comorbidities. Postoperative pulmonary hemodynamics were evaluated by right heart catheterization 1 month after PEA in 61 of the 66 PEA survivors. Perioperative data were collected from hospital records. Follow-up data, which were obtained by calling the patients or their primary physicians, were available for 74 patients (96% complete). The median and maximum follow-up periods were 5.6 years and 20 years, respectively.

Baseline patient characteristics are shown in Table 1. Fifty-five patients (56%) were female, and thus the gender distribution was female dominant. Twenty-four patients (31%) had a coagulation abnormality (antithrombin III deficiency, 5 patients; protein C or S deficiency, 5 patients; antiphospholipid syndrome, 9 patients), and 37 patients (48%) had a deep vein thrombosis. Most of the patients (79%) were in NYHA functional class III or IV, and all patients required home oxygen therapy. The mPAP was 47 ± 10 mm Hg, with 42% of the patients having mPAP values greater than 50 mm Hg. PVR was 868 ± 319 dyne · s · cm^{-5}, with 30% of the patients having PVR values greater than 1000 dyne · s · cm^{-5}.

On the basis of the location and morphology of the thromboembolic and vascular wall disease found at the time of surgery, the disease was classified as follows: type 1 (n = 61) consisted of fresh (acute) thrombus in the main lobar pulmonary arteries; type 2 (n = 12) consisted of intimal thickening and fibrosis with or without organized thrombus proximal to the segmental arteries; type 3 (n = 4) consisted of fibrosis, intimal webbing, and thickening with or without an organized thrombus within distal segmental arteries alone; and type 4 (n = 0) consisted of microscopic distal arteriolar vasculopathy without visible thromboembolic disease.[13]

PEA was performed through a median sternotomy with intermittent deep hypothermic circulatory arrest according to the procedure of University of California, San Diego group.[4,11,12] An inferior vena cava filter was put in place in 65 patients (84%). All PEA survivors received permanent anticoagulation therapy (Coumadin). Pulmonary vasodilator therapy (bosentan or sildenafil citrate [INN sildenafil]) was not routinely used, except for patients in NYHA functional class III.

Statistics

Results are expressed as mean ± SD. All analyses were performed with SPSS 18 software (IBM Corporation, Armonk, NY). The Wilcoxon signed-rank test was used for the comparison of preoperative and postoperative pulmonary hemodynamic data. Pulmonary hemodynamic data obtained by right heart catheterization 1 month after PEA were used for the calculation of postoperative mPAP or PVR, except in the case of patients who did not undergo postoperative right heart catheterization; for these patients, the data obtained before removal of the thermodilution catheter were used. Predictors of in-hospital mortality were analyzed by univariate analysis and multivariate stepwise logistic regression analysis. The univariate analysis was performed for continuous variables with a *t* test or a Mann-Whitney test and for categoric variables with the χ^2 test or the Fisher's Exact test. We calculated the incidence rates for all-cause mortality, disease-specific mortality, and adverse events, including disease-specific mortality and impaired functional status in NYHA functional class III, and we used the Kaplan-Meier method to estimate survivals. Univariate and multivariate stepwise analyses with the Cox proportional hazard model were performed to identify the risk factors for disease-specific death and adverse events. The optimal PVR cutoff point for in-hospital death and the optimal mPAP cutoff value for adverse events were determined with the aid of a receiver operating characteristic curve. Results are expressed as hazard ratios with 95% confidence intervals.

RESULTS

Early Results

There were 11 in-hospital deaths among the cohort studied (14%). The causes of death were as follows: right heart failure (n = 6), pulmonary hemorrhage (n = 2), cardiac tamponade (n = 2), and reperfusion lung edema (n = 1). With the exception of the 2 patients who died of cardiac tamponade, the other 9 patients had persistent pulmonary hypertension develop, and there were 5 patients who could not be weaned from cardiopulmonary bypass. Among the 66 PEA survivors, mPAP and PVR decreased (from 47 ± 10 mm Hg to 25 ± 10 mm Hg, $P < .0001$; from 868 ± 319 dyne · s · cm^{-5} to 313 ± 206 dyne · s · cm^{-5}, $P < .0001$; respectively), and cardiac index increased (from 2.5 ± 0.7 L/[min · m^2] to 3.1 ± 0.6 L/[min · m^2]; $P < .0001$). Comparisons between survivors and nonsurvivors in terms of preoperative data are shown in Table 2. In the multivariate analysis, only preoperative PVR (odds ratio, 1.003; 95% confidence interval, 1.001–1.005; $P < .01$) was an independent predictor of in-hospital death. To determine the cutoff point for the influence of preoperative PVR on in-hospital death, we performed receiver operating characteristic curve analysis. This revealed a preoperative PVR of 1052 dyne · s · cm^{-5} as the cutoff value for in-hospital death (area under the curve, 0.76; sensitivity, 0.64; specificity, 0.83).

Late Results

During the follow-up period, there were 10 all-cause deaths. Four deaths of right heart failure and 1 sudden cardiac death were regarded as being related to CTEPH. These patients exhibited NYHA functional class III symptoms as a result of persistence or worsening of pulmonary hypertension: 3 patients had persistent pulmonary hypertension with less than 10% decrease in PVR, and 2 patients had worsening of pulmonary hypertension despite early postoperative decrease in PVR (from 618 dyne · s · cm^{-5} to 386 dyne · s · cm^{-5} and from 1288 dyne · s · cm^{-5} to 507 dyne · s · cm^{-5}). Other causes of death included suffocation hematemesis, interstitial pneumonia, brain hemorrhage, and stroke. Among the operative survivors, clinical functional status improved markedly relative to the preoperative status. At the most recent follow-up at a mean of 6.5 years, 56 patients

TABLE 1. Baseline patient characteristics

Variable	Preoperative
Male (no.)	34 (44%)
Age (y, mean ± SD)	55 ± 11
Coagulation abnormality (no.)	24 (31%)
Deep vein thrombosis (no.)	37 (48%)
Insertion of inferior vena cava filter (no.)	65 (84%)
Duration of illness (mo, mean ± SD)	49.6 ± 40.4
New York Heart Association functional class (no.)	
I	0
II	16 (21%)
III	54 (70%)
IV	7 (9%)

(92%) were in NYHA functional class I or II, and 35 patients (63%) had been weaned from home oxygen therapy. Among 5 patients in NYHA functional class III, 4 patients had worsening of pulmonary hypertension at follow-up. Their PVR decreased from 795 ± 245 dyne · s · cm^{-5} to 398 ± 146 dyne · s · cm^{-5} early after surgery, but it rose again to 738 ± 214 dyne · s · cm^{-5} at follow-up.

Figure 1 shows freedoms from all-cause death, disease-specific death, and adverse events (including disease-specific death and impaired functional status, NYHA functional class III). The values for freedom from disease-specific death at 5 and 10 years were 84% and 82%, respectively, whereas those for freedom from adverse events were 78% and 70%.

We next sought to determine risk factors for late adverse events. In the individual variable model, age and postoperative mPAP and PVR were associated with adverse events; however, only postoperative mPAP was found to be significant in the multivariable analysis (hazard ratio, 1.12; 95% confidence interval, 1.03–1.21; $P < .01$). Receiver operating characteristic curve analysis revealed a postoperative mPAP of 34 mm Hg as the cutoff value for adverse events (area under the curve, 0.90; sensitivity, 0.80; specificity, 0.91).

Finally, the postoperative mPAP cutoff value was used to divide patients into 2 groups. There were no intergroup differences in any preoperative variables, although patients with a postoperative mPAP of at least 34 mm Hg had a trend toward higher preoperative mPAP values than did those with a postoperative mPAP lower than 34 mm Hg (50 ± 10 mm Hg vs 45 ± 10 mm Hg; $P = .10$). Comparison of freedom rates from late adverse events between the groups (Figure 2) revealed that patients with postoperative mPAP values lower than 34 mm Hg had good late outcomes. In that group, 10-year freedoms from disease-specific death and adverse events were 100% and 98%, respectively. In contrast, patients with postoperative mPAP values of at least 34 mm Hg had significant adverse events after PEA, and 10-year freedoms from disease-specific death and adverse events were 80% and 41%, respectively.

DISCUSSION

Medical treatment for CTEPH is palliative and unsatisfactory, but PEA is an effective therapeutic option that results in immediate and substantial improvements in pulmonary hemodynamics. This procedure is technically demanding, however, and requires proper patient selection and careful postoperative management, resulting in such relatively high in-hospital mortalities as 4.4% to 16%.[1,4,6,10,14,15] Although our overall in-hospital mortality of 14% may be relatively high, the rate was reduced to 7.5% in the last 40 cases with increasing surgical experience and refinements in operative and postoperative management.

Several risk factors for increased in-hospital mortality have been identified, including advanced age, severe pulmonary hemodynamic compromise, CTEPH type 3 or 4, distinct medical conditions involving other organ systems, and postoperative PVR greater than 500 dyne · s · cm^{-5}.[1,4,6,13,14,16] In this study, only high PVR was identified as a preoperative risk factor, with a PVR cutoff point of 1052 dyne · s · cm^{-5} for in-hospital death. Although other work has shown that postoperative PVR greater than 500 dyne · s · cm^{-5} may be a significant risk factor for in-hospital death,[4] we did not evaluate postoperative PVR because there were 5 patients who could not be weaned from cardiopulmonary bypass.

TABLE 2. Risk factors for hospital mortality

Variable	Survivors (n = 66)	Nonsurvivors (n = 11)	Univariate *P* value	Multivariate *P* value
Male (no.)	27 (41%)	7 (63%)	.20	—
Duration of illness (mo, mean ± SD)	47 ± 40	62 ± 39	.27	—
Mean pulmonary arterial pressure (mm Hg, mean ± SD)	46 ± 10	54 ± 9	.02	—
Pulmonary vascular resistance (dyne · s · cm^{-5}, mean ± SD)	825 ± 303	1124 ± 303	<.01	<.01
Cardiac index (L/[min · m2], mean ± SD)	2.5 ± 0.7	2.1 ± 0.5	.33	—
Chronic thromboembolic pulmonary hypertension type (no.)				
1	52 (87%)	8 (14%)		
2	12 (100%)	0 (0%)		
3	2 (50%)	2 (50%)	.10*	—

*Versus chronic thromboembolic pulmonary hypertension types 1 and 2.

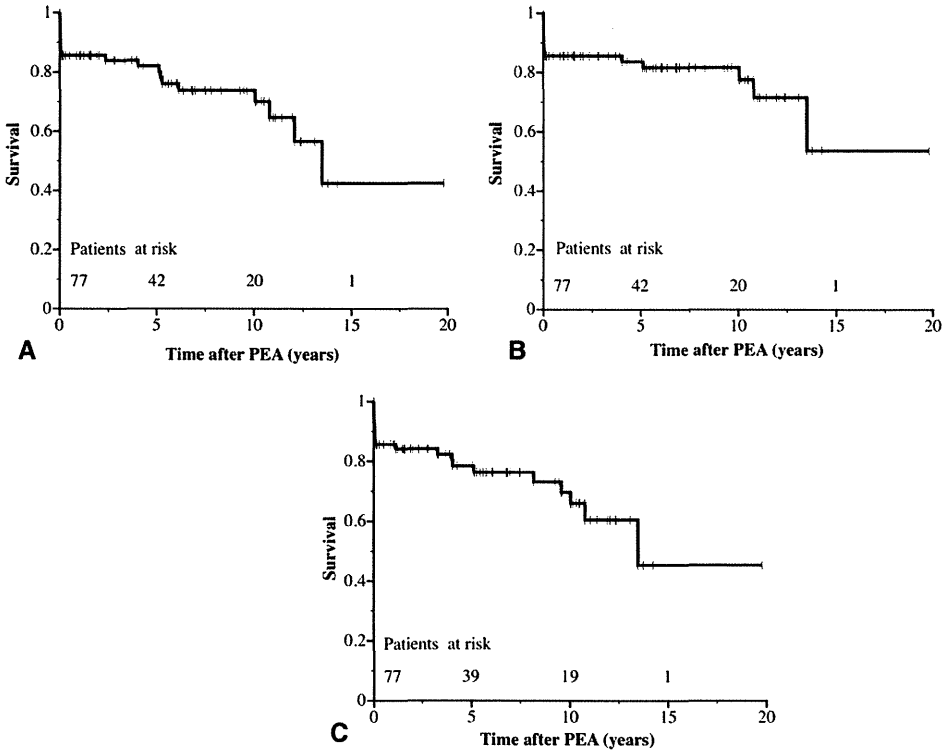

FIGURE 1. Overall Kaplan-Meier survival curves after pulmonary endarterectomy *(PEA)*. A, Freedom from all-cause mortality. B, Freedom from disease-specific mortality. C, Freedom from disease-specific mortality or New York Heart Association functional class III.

A previous study revealed that patients with a PVR greater than 1100 dyne · s · cm^{-5} had 6 times higher operative mortality (37%) than did those with a PVR lower than 1100 dyne · s · cm^{-5}.[16] Another study by Dartevelle and colleagues[1] showed that the mortality was 4% among patients with PVR lower than 900 dyne · s · cm^{-5}; however, this increased to 10% among those with PVR between 900 and 1200 dyne · s · cm^{-5} and to 20% among those with higher PVR. High PVR and CTEPH type 3 have been shown to be associated with persistent pulmonary hypertension, which is among the major complications after PEA and the leading cause of in-hospital death.[1,4] In a study by Thistlethwaite and associates,[13] patients with CTEPH type 3 disease had higher rates of perioperative mortality and morbidity and smaller decreases in PAP and PVR than did those with proximal disease (type 1 or 2). Likewise, Freed and colleagues[17] reported less improvement in pulmonary hemodynamics among patients with CTEPH type 3: 10 of their 17 patients with type 3 disease had postoperative persistent pulmonary hypertension, with mPAP values greater than 30 mm Hg. In the our study, it was not

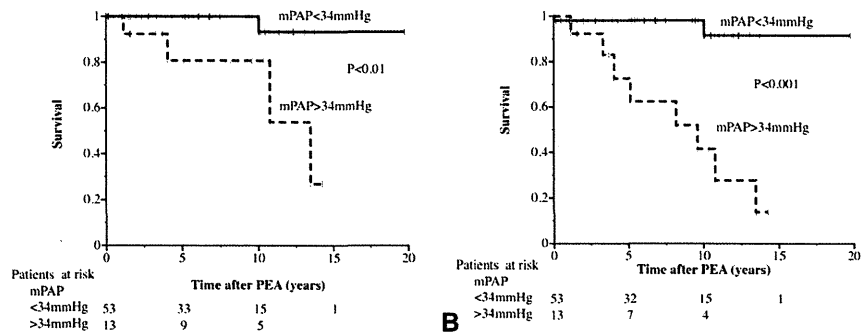

FIGURE 2. Kaplan-Meier survival curves after pulmonary endarterectomy *(PEA)* according to postoperative mean pulmonary arterial pressure *(mPAP)*. A, Freedom from disease-specific mortality. B, Freedom from disease-specific mortality or New York Heart Association functional class III.

conclusive whether CTEPH type 3 was associated with in-hospital mortality, because only a small number of patients had CTEPH type 3. Proper patient selection and careful perioperative management, however, are necessary when treating patients who have a high mPAP as a result of CTEPH type 3.

In addition to immediate improvements in pulmonary hemodynamics, PEA reportedly provides an excellent medium-term survival benefit, with 5-year survivals ranging from 75% to 89%.[6-9] In a long-term follow-up of 308 patients who underwent PEA between 1970 and 1994, a University of California, San Diego, group found that 75% survived beyond 6 years.[9] More recently, Corsico and coworkers[8] reported the late results obtained for 157 patients who underwent PEA between 1994 and 2006. They showed an 84% survival at 5 years, with a 30-day mortality of 11.5%. Our study, which reviewed the 20-year follow-up outcomes of patients who underwent PEA, has confirmed the persistent beneficial effect of PEA, as indicated by our late survival data. Indeed, 10-year survival was as high as 82% (Figure 1, *B*).

Patients with CTEPH are severely clinically compromised as a result of ventilation–perfusion mismatch and decreased cardiac output. In previous studies, more than 90% were in NYHA functional class III or IV, and most required oxygen therapy.[6,8,14] Despite that clinically unpromising background, PEA provided significant and sustained improvements in clinical symptoms, with more than 90% of patients being in NYHA functional class I or II and 2 thirds having been weaned from oxygen therapy at the latest follow-up.[6,8] In addition to prompt pulmonary hemodynamic improvement, PEA gradually improves gas exchange through a period of 6 months to 2 years after a temporal ventilation–perfusion abnormality caused by restrictive pulmonary functional impairment in response to surgical trauma, diffusion limitation in response to pulmonary edema, and a steal of perfusion from high-resistance nonobstructed segment to low-resistance newly perfused segements.[18,19] In our study, which was consistent with the previous results, only 63% of patients could be weaned from oxygen therapy, although 92% of patients were in NYHA functional class I or II. The discrepancy between excellent functional status and frequent oxygen therapy at follow-up can be explained by the fact that 10 of 21 patients with home oxygen therapy had a short follow-up period of less than 2 years.

Although a previous follow-up study found that persistent pulmonary hypertension and recurrent pulmonary embolism were the leading causes of late death,[9] the risk factors for late adverse events after PEA remain to be identified because the data on long-term survival are relatively scarce. In one of the few relevant reports, Bonderman and associates[15] showed that distinct medical conditions causing chronic infection or chronic inflammatory processes were risk factors for persistent pulmonary hypertension after PEA and were associated with both short- and long-term adverse outcomes. Freed and colleagues,[17] who reviewed medium-term follow-up results, showed that although persistent pulmonary hypertension with an mPAP value greater than 30 mm Hg led to impairments in both functional status and exercise capacity, it had no adverse impact on 5-year survival. Our long-term follow-up study showed that persistence and worsening of pulmonary hypertension were associated with late death or impairment of functional status and identified postoperative mPAP as a risk factor for late adverse events, whereas the preoperative risk factors for in-hospital death were not associated with late adverse events.

It has been shown that mPAP determines the prognosis of patients with medically treated CTEPH.[3] Actually, in previous studies, mPAP values greater than 30 mm Hg adversely affected survival in patients with medically treated CTEPH, whereas borderline pulmonary hypertension (20–26 mm Hg) was not associated with a poor prognosis.[3,20] In our study, a postoperative mPAP value of at least 34 mm Hg was found to be the cutoff value for late adverse events. To judge from these results, a high mPAP determines the prognosis of patients with CTEPH, whether the disease is treated surgically or medically, and thus a decrease of mPAP is the most important goal if we hope to achieve good late survival. In contrast to the poor outcomes among patients with persistent pulmonary hypertension, an excellent 10-year event-free survival (98%) was achieved among patients with resolved pulmonary hypertension (Figure 2). Our result indicates that PEA can be a curative and definitive surgical treatment and may be particularly important for patients with CTEPH, who are generally middle-aged (mean age around 52–57 years).[1,4,6,10,14,15]

Persistent pulmonary hypertension develops in 10% to 35% of patients who have undergone PEA, despite removal of sufficient proximal thromboembolic materials.[6,10,14,17] Pathologic examination of lung tissue in patients with CTEPH has shown that small vessel arteriopathy occurs not only in the area served by open proximal arteries but also in the area distal to occluded pulmonary arteries.[1,21,22] This small vessel arteriopathy causes progressive pulmonary hypertension and a symptomatic decline in the course of the CTEPH and is related to the development of persistent pulmonary hypertension after a successful PEA.[1,22] A reliable preoperative diagnostic tool for the involvement of distal arteriopathy has not been established[2,20,22]; however, patients who have a PVR that is disproportionately high with respect to the degree of proximal obstructions seen on pulmonary angiography are likely to have significant distal arteriopathy.[1,2,4] These patients have an elevated risk of persistent pulmonary hypertension and therefore may be selected for PEA only if a 50% reduction in PVR is predicted.[1]

In conclusion, in our experience PEA provided immediate and substantial improvements in pulmonary hemodynamics and had sustained favorable effects on long-term survival. High PVR was a significant independent risk factor for in-hospital death. Persistence and worsening of pulmonary hypertension were associated with late death or impairment of functional class, and postoperative mPAP was shown as a risk factor for late adverse events, with an mPAP value of at least 34 mm Hg being identified as the cutoff value for the prediction of such late adverse events.

References

1. Dartevelle P, Fadel E, Mussot S, Chapelier A, Hervé P, de Perrot M, et al. Chronic thromboembolic pulmonary hypertension. *Eur Respir J.* 2004;23:637-48.
2. Hoeper MM, Mayer E, Simonneau G, Rubin LJ. Chronic thromboembolic pulmonary hypertension. *Circulation.* 2006;113:2011-20.
3. Riedel M, Stanek V, Widimsky J, Prerovsky I. Longterm follow-up of patients with pulmonary thromboembolism. Late prognosis and evolution of hemodynamic and respiratory data. *Chest.* 1982;81:151-8.
4. Jamieson SW, Kapelanski DP, Sakakibara N, Manecke GR, Thistlethwaite PA, Kerr KM, et al. Pulmonary endarterectomy: experience and lessons learned in 1,500 cases. *Ann Thorac Surg.* 2003;76:1457-64.
5. Freed DH, Thomson BM, Tsui SS, Dunning JJ, Sheares KK, Pepke-Zaba J, et al. Functional and haemodynamic outcome 1 year after pulmonary thromboendarterectomy. *Eur J Cardiothorac Surg.* 2008;34:525-30.
6. Ogino H, Ando M, Matsuda H, Minatoya K, Sasaki H, Nakanishi N, et al. Japanese single-center experience of surgery for chronic thromboembolic pulmonary hypertension. *Ann Thorac Surg.* 2006;82:630-6.
7. Saouti N, Morshuis WJ, Heijmen RH, Snijder RJ. Long-term outcome after pulmonary endarterectomy for chronic thromboembolic pulmonary hypertension: a single institution experience. *Eur J Cardiothorac Surg.* 2009;35:947-52.
8. Corsico AG, D'Armini AM, Cerveri I, Klersy C, Ansaldo E, Niniano R, et al. Long-term outcome after pulmonary endarterectomy. *Am J Respir Crit Care Med.* 2008;15(178):419-24.
9. Archibald CJ, Auger WR, Fedullo PF, Channick RN, Kerr KM, Jamieson SW, et al. Long-term outcome after pulmonary thromboendarterectomy. *Am J Respir Crit Care Med.* 1999;160:523-8.
10. Condliffe R, Kiely DG, Gibbs JS, Corris PA, Peacock AJ, Jenkins DP, et al. Improved outcomes in medically and surgically treated chronic thromboembolic pulmonary hypertension. *Am J Respir Crit Care Med.* 2008;177:1122-7.
11. Jamieson SW, Auger WR, Fedullo PF, Channick RN, Kriett JM, Tarazi RY, et al. Experience and results with 150 pulmonary thromboendarterectomy operations over a 29-month period. *J Thorac Cardiovasc Surg.* 1993;106:116-27.
12. Jamieson SW, Kapelanski DP. Pulmonary endarterectomy. *Curr Probl Surg.* 2000;37:165-252.
13. Thistlethwaite PA, Mo M, Madani MM, Deutsch R, Blanchard D, Kapelanski DP, et al. Operative classification of thromboembolic disease determines outcome after pulmonary endarterectomy. *J Thorac Cardiovasc Surg.* 2002;124(6):1203-11.
14. Tscholl D, Langer F, Wendler O, Wilkens H, Georg T, Schäfers HJ. Pulmonary thromboendarterectomy—risk factors for early survival and hemodynamic improvement. *Eur J Cardiothorac Surg.* 2001;19:771-6.
15. Bonderman D, Skoro-Sajer N, Jakowitsch J, Adlbrecht C, Dunkler D, Taghavi S, et al. Predictors of outcome in chronic thromboembolic pulmonary hypertension. *Circulation.* 2007;115:2153-8.
16. Hartz RS, Byrne JG, Levitsky S, Park J, Rich S. Predictors of mortality in pulmonary thromboendarterectomy. *Ann Thorac Surg.* 1996;62:1255-60.
17. Freed DH, Thomson BM, Berman M, Tsui SS, Dunning J, Sheares KK, et al. Survival after pulmonary thromboendarterectomy: Effect of residual pulmonary hypertension. *J Thorac Cardiovasc Surg.* 2011;141:383-7.
18. Kapitan KS, Clausen JL, Moser KM. Gas exchange in chronic thromboembolism after pulmonary thromboendarterectomy. *Chest.* 1990;98:14-9.
19. Tanabe N, Okada O, Nakagawa Y, Masuda M, Kato K, Nakajima N, et al. The efficacy of pulmonary thromboendarterectomy on long-term gas exchange. *Eur Respir J.* 1997;10:2066-72.
20. Lewczuk J, Piszko P, Jagas J, Porada A, Wójciak S, Sobkowicz B, et al. Prognostic factors in medically treated patients with chronic pulmonary embolism. *Chest.* 2001;119:818-23.
21. Moser KM, Bloor CM. Pulmonary vascular lesions occurring in patients with chronic major vessel thromboembolic pulmonary hypertension. *Chest.* 1993; 103:685-92.
22. Galiè N, Kim NH. Pulmonary microvascular disease in chronic thromboembolic pulmonary hypertension. *Proc Am Thorac Soc.* 2006;3:571-6.

RESPIRATORY INVESTIGATION 50 (2012) 46–53

Contents lists available at SciVerse ScienceDirect

Respiratory Investigation

journal homepage: www.elsevier.com/locate/resinv

Original article

Evaluation of a learning system for endobronchial ultrasound-guided transbronchial needle aspiration

Yuichi Sakairi[a,*], *Fumie Saegusa*[b], *Shigetoshi Yoshida*[a], *Yuichi Takiguchi*[c], *Koichiro Tatsumi*[d], *Ichiro Yoshino*[a]

[a]*Department of General Thoracic Surgery, Chiba University Graduate School of Medicine, 1-8-1 Inohana, Chiba 260-8670, Japan*
[b]*Department of Endoscopic Diagnostics and Therapeutics, Chiba University Hospital, Chiba, Japan*
[c]*Department of Medical Oncology, Chiba University Graduate School of Medicine, Chiba, Japan*
[d]*Department of Respirology, Chiba University Graduate School of Medicine, Chiba, Japan*

ARTICLE INFO

Article history:
Received 16 January 2012
Received in revised form
15 March 2012
Accepted 20 March 2012
Available online 9 May 2012

Keywords:
Education
Endobronchial ultrasound
Learning curve
Lung cancer
Staging

ABSTRACT

Background: Endobronchial ultrasound-guided transbronchial needle aspiration (EBUS-TBNA) is an established modality for nodal staging in lung cancer; nevertheless, acquisition on effective fiberscope handling and puncture techniques remains challenging. Here, we present a novel EBUS-TBNA learning system protocol and evaluate the ability of physicians trained using this protocol to perform cytological diagnosis and histological sampling.

Material and methods: We designed a 5-step learning system as follows: (1) preparation, (2) probe insertion, (3) sonographic observation, (4) TBNA assistant, and (5) TBNA operator. Each trainee must accomplish the first 4 steps before beginning step 5. In step 5, EBUS-TBNA was performed in tandem by the trainee and supervisor. Diagnostic accuracy and success of histological sampling were recorded for each trial; results of the corresponding supervisor served as a control.

Results: All 11 trainees entered step 5 after completing steps 1–4 over 5–10 trials. A total of 308 nodes were punctured in step 5. The overall accuracy of cytological diagnosis was 91.2% among trainees, and the histological sampling success rate was 85.4%. The diagnostic accuracy increased from 85.4% to 93.9% ($p=0.027$) after 12 needle aspiration experiences. The sizes of nodes associated with success and failure were 13.6 and 11.1 mm ($p=0.001$), respectively.

Conclusions: Our EBUS-TBNA learning system provided a satisfactory educational pathway for trainees and can be used to improve accessibility of EBUS-TBNA.

1. Introduction

Endobronchial ultrasound-guided transbronchial needle aspiration (EBUS-TBNA) is reported to be a safe, less invasive, and highly diagnostic procedure for nodal staging (sensitivity, 88–93%; specificity, 100%) [1–5], and has recently become a standard modality for preoperative staging of lung cancer [6,7]. Additionally, we previously reported that histological samples of metastatic lymph nodes obtained by EBUS-TBNA can be applied to molecular analyses for detection of epidermal growth factor receptor (EGFR) mutations and the anaplastic lymphoma kinase (ALK) fusion gene [8,9], thereby providing information that enables the use of molecularly targeted therapy.

*Corresponding author. Tel.: +81 43 222 7171; fax: +81 43 226 2172.
E-mail address: y_sakairi1@chiba-u.jp (Y. Sakairi).

2212-5345/$ - see front matter © 2012 The Japanese Respiratory Society. Published by Elsevier B.V. All rights reserved.
http://dx.doi.org/10.1016/j.resinv.2012.04.002

Although EBUS-TBNA has become an essential technique for nodal staging and diagnosis, it remains inaccessible for some physicians. Moreover, some studies have shown that performing EBUS-TBNA requires specific training for fiberscope handling and that performing numerous TBNA procedures is required to overcome the learning curve [10–13]. However, training methods vary among institutions and have not been standardized.

Here, we present a protocol for a novel EBUS-TBNA learning system and provide evaluations on the abilities of trainees to make a satisfactory cytological diagnosis and to correctly sample histological tissue.

2. Material and methods

2.1. *Five-step learning system protocol*

We developed a 5-step learning system from our previous teaching experiences and applied it for clinical EBUS-TBNA instruction beginning in June 2010. This system consisted of the following 5 steps: (1) preparation, (2) probe insertion, (3) sonographic observation, (4) TBNA assistant, and (5) TBNA operator. The same supervisor evaluated each trainee at every step. The 2 basic rules of this learning system were: (1) each trainee must accomplish the first 4 steps before beginning step 5 and (2) trainees can experience the first 4 steps simultaneously when possible. These procedures were performed on patients who had given informed consent, with consideration for the patients' condition and ethical compliance. This research was approved by the ethics committee of Chiba University #1318. The essential elements of each step of this learning system are described below.

2.2. *Step 1: preparation*

During this phase, trainees were required to satisfactorily complete the following tasks:

- Prepare the examination table and know what is needed to perform EBUS-TBNA.
- Prepare the convex-probe fiberscope (XBF-UC260FOL8, Olympus, Tokyo, Japan).
- Load a balloon on the convex probe tip 3 times.
- Know how to clean the fiberscope.

In addition, the following elements were required to complete this step:

- Know how to operate the console (EU-C2000, Olympus).
- Learn the nodal echogram pattern.
- Operate the region of interest feature on the Doppler mode echogram.

After completing step 1, trainees became familiar with the basic equipment used in EBUS-TBNA and how to care for the equipment.

2.3. *Step 2: probe insertion*

Trainees were required to accomplish the following tasks by themselves:

- Insert a convex probe into the trachea in 3 cases.
- Aspirate sputum from the right and left main bronchus in 2 cases.

By completing step 2, trainees acquired the basic skill of fiberscope handling.

2.4. *Step 3: Sonography observation*

Trainees needed to accomplish the following tasks (5 cases were required for each task):

- Learn the positional relationships between nodes and great vessels.

(#4 R/2 R and superior vena cava, #10 R/4 R and azygos vein, #11 and pulmonary artery/vein, #4 L and aorta/pulmonary artery).

- Perform routine observation of the regional nodes from N1 to N3.
- Depict referred nodes that were noted on CT/PET images.

By completing step 3, trainees developed a better understanding of the anatomical structures in the mediastinum and hilum and were able to find the nodes systematically without assistance.

2.5. *Step 4: TBNA assistant*

Trainees were required to work as an assistant to the operator in 5 cases. Every trainee was required to maintain the fiberscope in an appropriate position, at an appropriate torque, and with a clear echoic view. By completing step 4, trainees were able to understand both the sequence of steps in the EBUS-TBNA procedure and the importance of appropriate assistance.

2.6. *Step 5: TBNA operator*

EBUS-TBNA was performed in tandem by the trainee and supervisor, who had performed more than 100 EBUS-TBNA procedures. TBNAs were always attempted by the trainee first, then by the supervisor. The puncture criteria were a length greater than 5 mm for the short axis or clinically suspected metastasis. The immediate diagnosis was made through on-site screening by a cytologist for every puncture and was used to decide the outcome of every trial. The trial was evaluated as "successful" when the assessable cytological sample was confirmed by on-site screening. The accuracy of cytological diagnosis was defined as the rate of concordance between the trainee and the corresponding supervisor. The histological sampling criterion was a gross visible core, and this was used to determine the success of histological sampling. The cytological diagnosis and success of histological sampling were recorded for each trial. Throughout this study, EBUS-TBNA

was performed without intubation, using a convex probe-EBUS and 22-gage dedicated needles in all trials. Lymph node stations and numbers were determined according to the seventh edition of the TNM classification for lung cancer [14].

2.7. *Threshold analysis from learning curve*

To evaluate the outcome of step 5, we designed a novel method for analyzing the learning curve (Fig. 1). First, a threshold was set for every 3 experiences in a pooled puncture database. The pooled database was divided into 2 categories according to training periods: the prethreshold and post-threshold periods. Data from each threshold point were included in the pooled data of the prethreshold period. Next, diagnostic rates and histological sampling rates were calculated for each prethreshold and post-threshold period. Finally, each value was tallied and plotted to depict a diagnostic or histological sampling learning curve.

2.8. *Statistical analysis*

Frequency analysis was performed using the chi-squared test (multinomial factors). The Mann–Whitney *U* test was applied to continuous data. General data analysis was conducted with JMP 9 (SAS Institute Inc., Cary, NC). All *p*-values were based on a 2-sided hypothesis; a *p*-value of less than 0.05 was considered to have statistical significance.

3. Results

3.1. *Entry*

From June 2010 to October 2011, 11 physicians applied to be trainees, all of whom were EBUS-TBNA beginners but had adequate experience in standard bronchoscopy. For steps 1–4, an average of 6.81±1.60 trials were required (range, 5–10 trials). During the study period, 146 patients underwent EBUS-TBNA and 308 punctures were performed. On average, 28 nodes were punctured by each trainee, and TBNA was performed 2.11±1.41 times per patient. Mediastinal nodes were punctured 207 times and hilar/peripheral nodes were punctured 101 times. The average nodal size (short axis) was 13.3 mm, and 42.2% (130/308) of nodes were 10 mm or smaller. These data are summarized in Table 1.

3.2. *Cytological diagnosis*

The pooled trainees' diagnostic rate throughout this study was 91.2% (281/308). In contrast, the pooled diagnostic rate of the supervisors was 99.7% (307/308). Diagnostic rates and average nodal sizes (of the short axis) are summarized in Table 2. The average node sizes for which trainees could and could not establish a diagnosis were 13.4 and 12.8 mm, respectively; this difference was not significant ($p=0.67$).

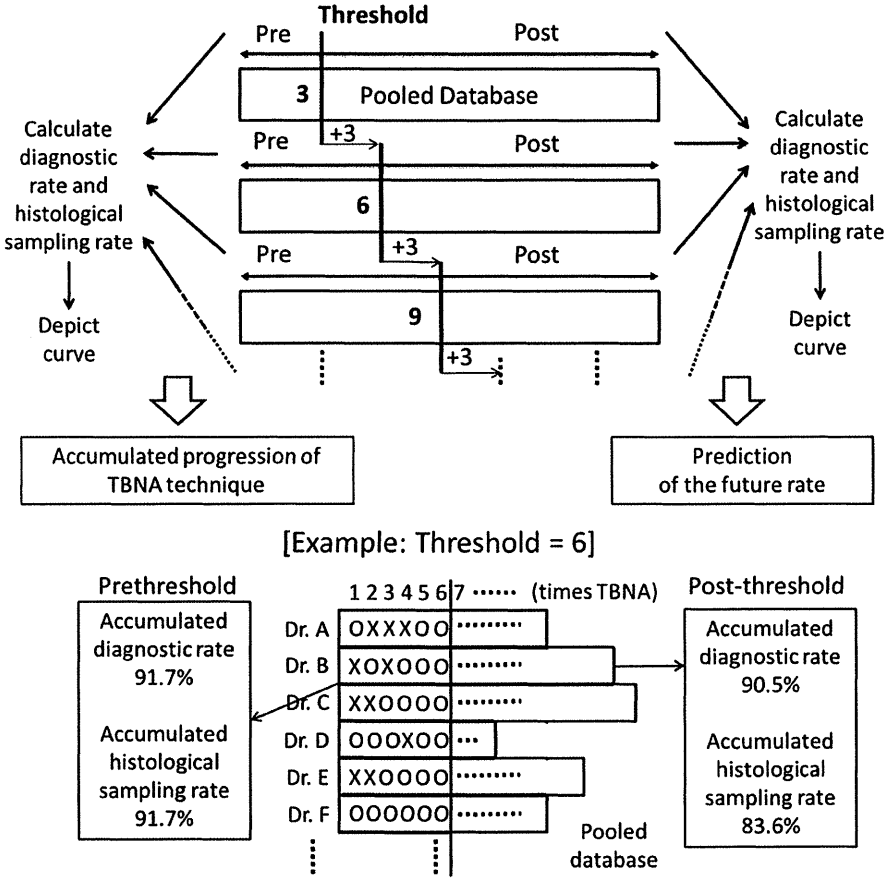

Fig. 1 – Threshold analysis. A comprehensive scheme for the threshold analysis.

3.3. Histological sampling

The trainees' histological sampling rate throughout this study was 85.4% (263/308), while the histological sampling rate of the supervisors was 99.7% (307/308). Histological sampling rates and average nodal sizes (of the short axis) are also summarized in Table 2. The average node sizes for which trainees could and could not obtain a histological core were 13.7 and 11.1 mm, respectively; this difference was significant ($p=0.0013$).

3.4. Nodal size and outcomes

With respect to nodal size, the diagnostic rate was consistently high, with values ranging from 88.9% (for nodes less than 5 mm along the short axis) to 94.1% (for nodes 25 mm or larger; Fig. 2). However, the histological sampling rate for nodes smaller than 5 mm was low (55.6%). Enlarged nodes (10 mm or more along the short axis, $n=178$) were associated with a cytological diagnostic rate and histological sampling rate of 91.0% and 90.4%, respectively; this difference was not significant ($p=0.65$). In contrast, for small nodes (less than 10 mm along the short axis, $n=130$) these rates were 91.5% and 79.2%, respectively, representing a statistically significant difference ($p=0.0054$).

Table 1 – Summary of entry data and puncture stations.

Parameter	Demographic data	
Trainees	11 physicians	
Learning step	Number of trials	Range
Step 1	3.63±0.8	3–5
Step 2	3.18±0.4	3–4
Step 3	5	5
Step 4	5	5
Step 1 to 4	6.82±1.6	5–10
Patients	146	
TBNA	308 times	
	Average 28 nodes/trainee	
	2.11±1.41 times/patient	
Nodal size in short axis		
Average	13.3±6.77 mm	
Range	3.4–34.0 mm	
<10 mm	42.2% (130/308)	
Nodal station	N	(%)
Mediastinum	207	(67.2)
#2R	8	(2.6)
#4R	72	(23.4)
#4L	30	(9.7)
#7	97	(31.5)
Hilar and peripheral	101	(32.8)
#10L	3	(1.0)
#11L	36	(11.7)
#11s	35	(11.4)
#11i	22	(7.1)
#12	5	(1.6)

3.5. Nodal location and outcomes

The relationships between outcome and nodal location were analyzed (Table 3). Both the diagnostic and histological sampling rates were relatively lower for #4 L. The chance of failure for these procedures was consistently high at 16%, even in educated trainees (i.e., those who had performed needle aspiration at least 12 times). For the other stations, the failure rate progressively decreased in educated trainees.

3.6. Threshold analysis

The accumulated diagnostic rates in the prethreshold and post-threshold periods for each threshold point are depicted as a curve in Fig. 3A and B. The curve of the prethreshold data (Fig. 3A) shows that the diagnostic rate initially decreased

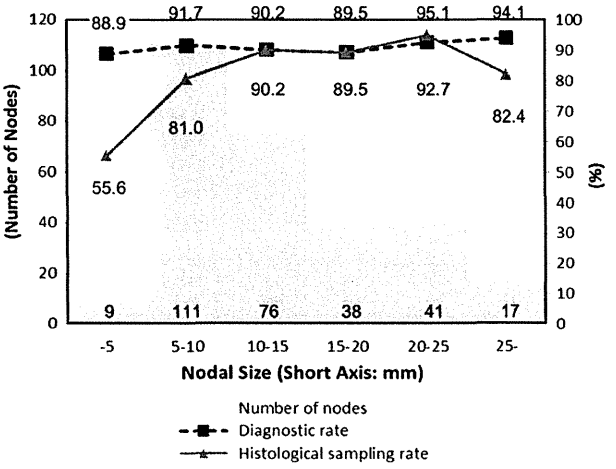

Fig. 2 – Nodal size distribution and diagnostic/histological sampling rates. Diagnostic rates and histological sampling rates for each nodal size (grouped in 5-mm increments).

Table 2 – Diagnostic rates, histological sampling rates, and nodal sizes.

Trainee	Supervisor	Diagnosis	Histological sampling	Average nodal size (short axis: mm)	
				Dx	Hx
Success	Success	281	263	13.4	13.7
Success	Failure	1	1		
Failure	Success	27	45	12.8	11.1
Failure	Failure	0	0		
p value				0.67	0.0013

Dx: Diagnosis.Hx: Histological sampling.